NASA Technical Paper 1776

Simulator Study of Conventional General Aviation Instrument Displays in Path-Following Tasks With Emphasis on Pilot-Induced Oscillations

James J. Adams

DECEMBER 1980

NASA

NASA Technical Paper 1776

Simulator Study of Conventional General Aviation Instrument Displays in Path-Following Tasks With Emphasis on Pilot-Induced Oscillations

James J. Adams
Langley Research Center
Hampton, Virginia

National Aeronautics
and Space Administration

**Scientific and Technical
Information Branch**

1980

SUMMARY

A study of the use of conventional general aviation instruments by general aviation pilots in a six-degree-of-freedom, fixed-base simulator has been conducted. The tasks performed were tracking a very high-frequency omnirange (VOR) radial and making an instrument landing system (ILS) approach to landing. A special feature of the tests was that the sensitivity of the displacement indicating instruments, the radio magnetic indicator (RMI), the course deviation indicator (CDI), and the horizontal situation indicator (HSI) was kept constant at values corresponding to 5 n. mi. and 1.25 n. mi. from the station. Both statistical and pilot-model analyses of the data were made.

Test results show that performance in path-following tasks improved with increases in display sensitivity until the highest test sensitivity setting was reached. At this maximum test sensitivity value, which corresponds to the sensitivity existing at 1.25 n. mi. from the ILS glide slope transmitter, tracking accuracy was no better than at 5 n. mi. from the transmitter, and the pilot-aircraft system exhibited a marked reduction in damping. In some cases, a pilot-induced, long-period unstable oscillation occurred.

INTRODUCTION

General aviation accident reports (ref. 1) indicate that many accidents occur during terminal area flying operations in instrument meteorological conditions. A factor which may contribute to this accident rate is the role played by the instrument configurations and sensitivities in the pilot-aircraft system stability. Pilot response studies and pilot-modeling efforts have shown that the pilot does respond much like a linear feedback control mechanism when controlling an aircraft; therefore, the pilot-aircraft system can be analyzed as a linear system, and the system stability characteristics can be determined. Aircraft are designed so that in most cases this system stability is positive (damped), but occasions do arise when the system is unstable. Pilot-induced unstable oscillations have been an item of study for some time. A recent summary study is given in reference 2. Until recently, these studies have usually centered around short-period (around 2 to 3 sec) instabilities that occur at high dynamic pressure, where the associated divergence of angle of attack can result in structural failure. Long-period unstable oscillations can also occur which involve only small variations in angle of attack or sideslip, but large displacements from the desired flight path of the aircraft. Evidence of such long-period instabilities may be found in measurements made during simulated instrument landing approaches. However, in these instances, the oscillations usually do not have time to become fully developed before the pilot breaks out of the weather conditions and stable visual flight is restored. The present study emphasizes the existence of these long-period instabilities by using special test techniques made possible by the flexibility of the simulator computer and relates them to conventional general aviation instrument display configurations.

SYMBOLS

G_u, G_v, G_w	gust spectrum transfer functions
h	altitude, m
K_h, K_y	pilot-model gains, rad/m
$K_\theta, K\psi, K\phi$	pilot-model gains, dimensionless
L_u, L_v, L_w	gust characteristic wavelengths, m
m	mass, kg
P	probability of being incorrect in assuming that the hypothesis that the scores are equal is wrong
p,q,r	roll, pitch, and yaw angular rates, rad/sec
s	Laplace operator, per sec
T_R	aircraft roll time constant, sec
T_S	aircraft spiral time constant, sec
V	velocity, m/sec
y	lateral distance, m
α, β	angles of attack and sideslip, rad
δ_a, δ_e	aileron and elevator deflections, rad
λ	real root, per sec
ω_C, ζ_C ω_{DR}, ζ_{DR} ω_ϕ, ζ_ϕ ω_y	frequencies, rad/sec, and damping ratios for pilot model-aircraft system mode of motion
ψ, θ, ϕ	yaw, pitch, and roll angles, rad
$\sigma_u, \sigma_v, \sigma_w$	gust transfer function amplitudes, m/sec

Nondimensional stability derivatives:

$C_{L\delta_e}$	lift coefficient due to elevator deflection
$C_{l\beta}$	rolling-moment coefficient due to sideslip
$C_{n\beta}$	yawing-moment coefficient due to sideslip

$C_{n_{\delta_a}}$ yawing-moment coefficient due to aileron deflection

C_{y_β} side-force coefficient due to sideslip

Dimensional stability derivatives:

F_{Y_p} side force due to rolling velocity, N-sec

F_{Y_r} side force due to yawing velocity, N-sec

F_{Y_β} side force due to sideslip, N

g gravity, m/sec^2

I_X, I_Z moment of inertia, $kg-m^2$

I_{XZ} product of inertia, $kg-m^2$

M_{X_p} rolling moment due to roll velocity, N-m-sec

M_{X_r} rolling moment due to yawing velocity, N-m-sec

M_{X_β} rolling moment due to sideslip, N-m

$M_{X_{\delta_a}}$ rolling moment due to aileron deflection, N-m

M_{Z_p} yawing moment due to rolling velocity, N-m-sec

M_{Z_r} yawing moment due to yawing velocity, N-m-sec

M_{Z_β} yawing moment due to sideslip, N-m

$M_{Z_{\delta_a}}$ yawing moment due to aileron deflection, N-m

Abbreviations:

CDI course deviation indicator

def deflection

HSI horizontal situation indicator

IFR Instrument Flight Rules

ILS instrument landing system

RMI radio magnetic indicator

VOR very high-frequency omnirange

Subscripts:

c	command
DR	Dutch roll
H	heading
R	roll
S	spiral
ϵ	error

A dot over symbol indicates derivative with respect to time.

EXPERIMENTAL PROCEDURES

A six-degree-of-freedom, fixed-base simulation effort was undertaken to examine pilot response to conventional general instruments. The tasks involved in these tests were to track a given radial to a very high-frequency omnirange (VOR) station or to make an instrument landing system (ILS) approach to landing. A special feature of these tests was to maintain constant sensitivity of the displacement indicating instruments during a given run. In the actual situation of navigating to a VOR station or making an approach to an ILS station, the sensitivity of the displacement instruments, with respect to linear displacement from the desired path, does change with linear distance from the station. This effect results because the display systems actually show an angular measure of displacement. That is, they show the angle between a line from the aircraft to the station and the line representing the desired path. On the other hand, the pilot has control of linear displacement. For any given input on the part of the pilot, the same displacement output results regardless of aircraft distance from the station. As a result, to the pilot, the displacement-indicating instruments appear to undergo an increase in sensitivity as the aircraft approaches the station.

The purpose of the present tests was to obtain an accurate measure of the pilot's response to the displacement instruments under the condition of constant sensitivity. This procedure eliminates the confounding effect of changing sensitivity on data analysis. The sensitivity was kept constant by the simple procedure of using a constant range to the station, even though the aircraft was traveling at some given airspeed. The sensitivities chosen for study were those that correspond to 5 n. mi. and 1.25 n. mi. from the station. At 1.25 n. mi. from the ILS glide slope station, the aircraft would still be at an altitude of 120 meters; thus the aircraft could still be expected to be in instrument conditions.

The lateral course deviation signal used when tracking to the VOR station was computed as follows:

$$\text{Lateral deviation signal} = \tan^{-1} \frac{\Delta y}{9300} \quad \text{(for the 5 n. mi. range)}$$

or

$$\text{Lateral deviation signal} = \tan^{-1} \frac{\Delta y}{2320} \quad \text{(for the 1.25 n. mi. range)}$$

A gain was put on this signal so that a 10° deviation would register as a full deflection on the instrument. While controlling this lateral signal, the pilot was also required to control altitude at 610 meters and airspeed at 135 knots.

The signals used for the ILS landing approach were

$$\text{Lateral deviation signal} = \tan^{-1} \frac{\Delta y}{9300 + 2140}$$

or

$$\text{Lateral deviation signal} = \tan^{-1} \frac{\Delta y}{2320 + 2140}$$

where the extra 2140 meters is the additional distance from the glide slope station to the localizer station. That is, when the distance from the ILS station is referred to as either 5 n. mi. or 1.25 n. mi., this value represents the distance from the aircraft to the glide slope ground impact point. The localizer station is an additional 2140 meters away from the aircraft. A gain was put on this signal so that a 2.5° deviation would move the localizer needle to full deflection. The ILS signal is 4 times more sensitive than the VOR signal.

The vertical needle deflection was

$$\text{Vertical needle deflection} = \tan^{-1} \frac{\Delta h}{9300}$$

or

$$\text{Vertical needle deflection} = \tan^{-1} \frac{\Delta h}{2320}$$

A gain was put on this signal so that a 0.7^{o} deviation would move the glide slope needle to full deflection. During an ILS approach, the pilot had to control both glide slope and localizer while maintaining 85 knots airspeed.

Three different displacement indicating instruments were studied: the course deviation indicator (CDI), the horizontal situation indicator (HSI), and the ratio magnetic indicator (RMI). Both the CDI and the HSI are designed to operate in conjunction with either VOR or ILS stations; the RMI is designed to operate only with VOR stations. With the RMI, the angular deviation signal described in the preceding section was applied directly to the station homing needle. Figure 1 shows the location of each of these instruments in the instrument panel of the simulator. Each displacement instrument was tested separately. When one of them was active, the other two were inactive. Along with each displacement indicating instrument, the attitude indicator, the directional gyro indicator, and the airspeed, altimeter, and rate-of-climb indicators were also operating.

The subjects had no duties to perform other than controlling to the desired flight path. Prior to the tests, the subjects were informed that the test runs were 3 minutes long, and were asked to direct their full attention to maintaining path control. Upon completion of the tests, all subjects reported that they had concentrated solely on this control objective.

Subjects

Ten subjects were used in these tests. In experience, they ranged from pilots who flew their aircraft only occasionally and who were either in the process of obtaining or had just recently received their instrument ratings, to professional test pilots. All the subjects had considerable simulator experience. The subjects' age and accumulated flight hours are listed in the following table:

Number	Subject initials	Age	Total flight hours	IFR flight hours	IFR hours in last 12 months
1	DH	22	200	5	2
2	MM	53	230	50	25
3	JS	40	250	62	16
4	JR	44	360	66	1
5	HV	31	1000	300	30
6	SS	25	1400	75	75
7	HB	43	2500	50	2
8	SH	36	2500	500	15
9	PB	39	3500	600	15
10	PD	45	6100	2100	25

Test Procedures

These 10 subjects had all taken part in previous test programs on the general aviation flight simulator at the Langley Research Center and, therefore, were familiar with the response of the simulator. They were, nevertheless, given a warmup session at the beginning of each test day. Tests of the CDI at 5 n. mi. and 1.25 n. mi. from the VOR station with an initial lateral error and no winds were conducted on the first day. Next, the same conditions with winds were tested. Then, the same series of tests were run with the HSI instrument. Finally, the same eight runs were made using the ILS station. On the second test day, the order of the CDI and HSI instruments was reversed, and then the block of four runs was performed using the RMI.

Aircraft Model

A realistic six-degree-of-freedom, nonlinear model was used to simulate a typical high-wing, four place, single-engine, general aviation airplane in this study. In addition to nonlinear kinematics, the following nonlinear aerodynamic factors and other special features were included in the simulation:

1. Nondimensional lift and drag coefficients were a function of α^2 as well as α.

2. Nondimensional stability coefficients C_{y_β}, $C_{L_{\delta_e}}$, C_{l_β}, $C_{n_{\delta_a}}$, and C_{n_β} were a function of α.

3. Asymmetric forces and moments as a function of thrust coefficient were included.

4. A hydraulic control loader that provided control forces as a function of aerodynamic hinge moments was included.

5. A sound system that provided realistic engine and airstream noise was included.

The dynamic response of this simulation model to step control inputs at the two values of airspeed (85 and 135 knots) that were used in the tests are shown in figures 2 and 3. Figure 2(a) shows the short-period response to a 0.02-rad elevator step at the two values of airspeed. The response is well damped and the frequencies are reasonably high, i.e., on the order of 6 rad/sec. Figure 2(b) shows the phugoid response to an initial out-of-trim angle of attack; the phugoid was found to be stable with periods of 55 and 30 seconds.

The lateral dynamic responses at the two airspeeds are shown in figure 3. The Dutch roll mode is fairly well damped and has frequencies of 3 and 2 rad/sec. Figure 3 also depicts the large effect of the adverse yaw on the yaw rate response. For further insight into the lateral response, the lateral linear perturbation equations of motion were written, and the aircraft lateral response characteristics were analytically determined. The linear equations are

$$\dot{\beta} = \frac{F_{Y_\beta}\beta + F_{Y_p}p + F_{Y_r}r}{mV} + \frac{g}{V}\phi - r$$

$$\dot{p} = \frac{M_{X_\beta}\beta + M_{X_p}p + M_{X_r}r + M_{X_{\delta_a}}\delta_a + \left(M_{Z_\beta}\beta + M_{Z_p}p + M_{Z_r}r + M_{Z_{\delta_a}}\delta_a\right)\frac{I_{XZ}}{I_Z}}{I_X - \frac{I_{XZ}^2}{I_Z}}$$

$$\dot{r} = \frac{M_{Z_\beta}\beta + M_{Z_p}p + M_{Z_r}r + M_{Z_{\delta_a}}\delta_a - \dot{p}I_{XZ}}{I_Z}$$

At 85 knots,

$$\dot{\beta} = -0.229\beta + 0.0065r - 0.0162p + 0.225\phi - r$$

$$\dot{p} = -6.95\beta + 1.10r - 4.82p - 8.53\delta_a$$

$$\dot{r} = 2.85\beta - 0.725r - 0.436p + 0.216\delta_a$$

At 135 knots,

$$\dot{\beta} = -0.324\beta + 0.0065r - 0.0162p + 0.225\phi - r$$

$$\dot{p} = -18.85\beta + 1.71r - 7.50p - 20.7\delta_a$$

$$\dot{r} = 7.91\beta - 1.13r - 0.677p + 0.527\delta_a$$

The lateral response characteristics, as determined from these equations, are

At 85 knots,

$T_S = 44$ sec $\quad T_R = 0.2$ sec $\quad \omega_{DR} = 1.95$ rad/sec $\quad \zeta_{DR} = 0.208$

At 135 knots,

$T_S = 70$ sec $\quad T_R = 0.13$ sec $\quad \omega_{DR} = 3.16$ rad/sec $\quad \zeta_{DR} = 0.203$

These analytical results for the Dutch roll agree with the results noted for the time histories; the other results provide further information on the spiral and roll time constants.

Wind Input

In some of the tests conducted as part of this experiment, wind inputs were used as forcing functions. These wind inputs consisted of a steady cross wind of 1.22 m/sec in magnitude and a random input used to represent gusts. Three gust inputs v_g, u_g, w_g were generated using random-number generators and filters based on the Dryden gust model. The filters were

$$G_u(s) = \sigma_u \left[\frac{1}{s + \frac{1}{L_u}} \right]$$

$$G_v(s) = \sigma_v \left[\frac{s + \frac{1}{3}\frac{V}{L_v}}{s + \frac{V^2}{L_v}} \right]$$

$$G_w(s) = \sigma_w \left[\frac{s + \frac{1}{3}\frac{V}{L_w}}{s + \frac{V^2}{L_w}} \right]$$

The scale lengths were

$$L_u = L_v = h \qquad \text{(for } h \geq 535 \text{ m)}$$

$$L_u = L_v = 44h^{1/3} \qquad \text{(for } h < 535 \text{ m)}$$

$$L_w = h$$

The values of the individual gust amplitudes were set to occur in the following relative values:

$$\sigma_u = 1.12 \qquad \sigma_v = 1.18 \qquad \sigma_w = 1.16$$

During the tests, the overall gust amplitude was adjusted so that the average gust root mean square was 1.22 m/sec at an altitude of 535 meters. The mean value of the gusts was zero.

Method of Analysis

A statistical analysis was conducted by measuring the mean and standard deviation of the lateral and vertical errors of the runs made with the wind disturbances. A t-test was conducted between the different range conditions with each instrument, and between the different instruments at each range condition to determine the level of significance of the differences.

A pilot-model analysis was performed to provide time histories for comparison with the time histories obtained in the simulation exercise. Block diagrams of the pilot-model-aircraft system are shown in figure 4. Decoupled and linearized diagrams are shown for the separated lateral and longitudinal system for simplicity. The pilot is represented by simple gains in the outer displacement loops (y and h) and, for lateral control, in the ψ loop. The inner loops ϕ and θ contain a gain and a lag function that represent the characteristics of the response used by the pilot to put the control manipulator in the desired position. The second-order form for this response is used because the subsystem represented does involve an inertia, i.e., the manipulator inertia plus the pilot's arm. A perfect-square form is used to represent the critically damped response employed. The 0.2-sec lag time constant used is a preferred lag time constant. It is a long time constant compared with the 0.04-sec time constant that a pilot can use in a simple control task when required by the system stability considerations. Therefore, the 0.2-sec lag time constant represents an undemanding response as well as the value that pilots use in complicated, multiloop control tasks, where much of the pilot's attention must be directed to reading the instruments.

A lead can also be included in the pilot-model inner loop and would be included if called for by the system stability compensation requirements. This lead would represent the pilot's response to the rate of change of the inner-loop variable. Lead time constants of 1 sec have been measured in single-loop control tasks. However, in complex, multiloop control tasks, the pilot has very little time available to differentiate the inner-loop variable display. The present study assumes that no inner loop lead is present.

The relations between the aircraft control inputs δ_a and δ_e and the rate of change of the inner loop variables p and q are shown as blocks (labeled "aircraft") in the diagram (fig. 4). These blocks represent complex relations involving many integrations, all of which are interconnected as defined by the equations of motion. The complexity of these relations admits the possibility of large variations in responses of p and q to δ_a and δ_e, which can have a decided influence on the total system response. Investigation of these aircraft response effects is covered by an extensive body of published handling-qualities studies. References 3 and 4 cover this area of research from a pilot-model viewpoint.

The present study is concerned with the dynamic phase lags which are present in the relations of the variables that the pilot is asked to regulate. These phase lags are emphasized in the block diagram (fig. 4) by showing the integrations that exist between these variables. The 90° phase lag between θ (or γ) and h, for vertical control, and the 90° between ϕ and ψ and ψ and y, for lateral control, indicate that the pilot must coordinate his response to these variables to achieve a satisfactory system response. The pilot's ability to provide this coordination is related to the configuration and sensitivity of the display of these variables. This ability is the focal point of the present investigation. The pilot model described in the block diagram was used to obtain time histories that could be used for comparison with the records obtained from the test subjects. These system responses were obtained using the pilot model in conjunction with the six-degree-of-freedom nonlinear aircraft model. Both a lateral pilot model and a vertical pilot model were used. The vertical pilot model was used to maintain a constant altitude. Analytically determined lateral system characteristics were also obtained using the linear pilot model, the linear lateral perturbation equations presented previously, and the following linearized kinematic relations:

$$\dot{\psi} = \frac{g}{V}\phi$$

$$\dot{y} = V\psi$$

To illustrate the lateral response of the modeled pilot-aircraft system, sample time histories obtained with typical pilot-model gains and the aircraft simulation model are shown in figures 5 to 7. These figures also illustrate the effect of the two different airspeeds used in the study, the effect of the remnant term in the pilot model, and the effect of the wind disturbance.

The time histories of figure 5, for which the pilot model contained no remnant term, show a stable system. The analytically determined system characteristics, shown in table I, also indicate that the system is stable. The table indicates a system response which contains four modes of motion. The high-frequency control mode is derived from the pilot-model inner-loop characteristic $(0.2s + 1)^2$ or $(s + 5)^2$. In the complete system, this mode is altered slightly. This mode of motion is not noticeable in the time histories. The next lower frequency mode is the aircraft Dutch roll mode, which also is altered slightly by the additional loop closures of the complete pilot-model-aircraft system. The next lower frequency is an oscillatory mode derived from the combination of the zero-value heading root and the lower value roll root. This mode of motion is the oscillatory mode that appears in the time histories. The final mode of motion is derived from the zero-value lateral displacement root and the higher roll root. In this sample case, the two roots involved remain real roots rather than combining into an oscillatory model. The lower real root and the roll-heading oscillatory root determine the shape of the time history response.

The differences in the time histories for the two airspeeds correspond to the differences in the roots (table I) for the same two airspeeds. Since the systems are stable in each case, the time histories converge to a constant steady-state value. The asymmetrical-engine-thrust terms that are included in the aircraft simulator model cause the nonzero value for the steady state.

The migration of the system roots that occurs as the pilot-model feedback loops are closed is illustrated in the second part of table I for the 85-knot airspeed case. With no loops closed ($K_\phi = 0$, $K_\psi = 0$, $K_y = 0$), the system consists of the unchanged Dutch roll, spiral, and roll roots. When the bank angle loop is closed ($K_\phi = -0.16$), the spiral root takes on a large negative change and the roll root is reduced in value. When the heading loop is closed ($K_\phi = -0.16$, $K_\psi = 1.25$), the lower roll root and the heading root combine to form a stable oscillatory root. When the displacement loop is closed, the system takes on the characteristics described in the previous paragraph.

Next, a representative pilot remnant was added to the pilot model. This remnant was generated by passing a white-noise random signal through a second-order filter identical to the pilot-model characteristic:

$$\left[\text{Remnant} = \frac{K_n}{(0.2s + 1)^2}(\text{random signal})\right]$$

and adjusting the gain K_n to provide a typical pilot remnant amplitude. The effect of adding the remnant (shown in fig. 6) is to make the Dutch roll mode and the roll-heading mode of motion much more visible in the system response. With the remnant signal included, the system response now converges to an approximately constant-amplitude oscillatory steady-state condition rather than to a constant-value steady state. The frequencies of different modes of motion are detectable in the time histories, and the amplitude of the different modes is dependent on the frequency and damping of the modes and the amplitude of the remnant input.

The effect of adding the wind disturbance is shown in figure 7. The steady-cross-wind component of the wind more than offsets the asymmetric thrust moments and causes a positive-value bias in the displacement time history. The random component of the wind increases the steady-state oscillatory amplitude in the system response. Again, the amplitude of the steady-state oscillation is a function of the frequency and damping of the system modes of motion.

RESULTS

Statistical Analysis

Time histories typical of the results obtained in the study are shown in figures 8 and 9. The lateral and vertical deviations from the desired path for runs in which the wind disturbance was included are shown in figure 8. The

lateral deviation for runs in which there was an initial lateral error, but no winds, is shown in figure 9. The initial lateral error was set so that the initial navigation display needle deflection was always the same, approximately one-third full deflection.

Although the sensitivity of the CDI and HSI are approximately equal, the sensitivity of the RMI to lateral displacement error is much less than that of either the CDI or the HSI. The time history records, especially the records with an initial lateral error, demonstrate that the frequency of the pilot-aircraft system is very low with the RMI. With the CDI and HSI, several cycles of the dominant oscillatory mode take place in the 3-minute time span of the test. With the RMI the system frequency is so low that not even one complete cycle occurs within the time of the test. It was concluded from those observations that path following with the RMI is much less accurate than with either the CDI or the HSI. Furthermore, the mean and standard deviation that are measured under the conditions of the test do not accurately describe the system for the RMI; for this reason, the RMI tests were not carried out with the same degree of effort as for the CDI and HSI. Only one set of measurements with each subject was made with the RMI.

The standard deviations and means for the lateral displacement errors are presented in tables II and III. Since the sensitivity of the lateral displacements increases with decreases in range to the station, performance may be expected to improve at shorter range. This range effect is very clear for the en route VOR data for the CDI and HSI. The average standard deviation and mean for each of these instruments show obvious reductions in scores in going from the 5 n. mi. range to the 1.25 n. mi. range. The scores for the RMI did not vary. In the tests with the ILS station, neither the standard deviation nor the mean showed any significant change for the two ranges. Additional t-test comparisons of the different pairs of data were made and show that the differences noted before were significant. The P-values are listed in tables II to V. A P-value of less than 0.025 can be used to indicate a significant difference. Except for the mean obtained with the HSI tracking to the VOR station, the P-values show that the differences noted before are indeed significant.

The different instruments were also compared at the same tracking range. When tracking to the VOR station, the best scores were obtained with the HSI, the second best with the CDI, and the worst with the RMI in both standard deviation and mean (tables II(a) and III(a)). The t-tests on the different pairs of data (tables II(b) and III(b)) confirm that these differences are significant at the 0.025 level except in the case of the means for the pairs CDI-RMI at 5 n. mi. and CDI-HSI at 1.25 n. mi. The lack of significance in the first of these two cases may only reflect insufficient data for the RMI.

When tracking to the ILS station, the CDI and HSI were significantly different at the 5 n. mi. range for standard deviation but not for the mean; HSI displayed the better scores. At 1.25 n. mi. there were no significant differences between the CDI and the HSI. The time histories show that with each of these instruments the lateral displacement becomes very erratic at the short range. A more detailed analysis of this situation is presented in a subsequent section of this study.

Standard deviations and means were also measured for vertical control (tables IV and V). When tracking to the VOR station, the pilot controlled altitude by referring to the altimeter and attempting to hold a 610-meter altitude. With this configuration there is no change in sensitivity in the display of altitude error with change in range, and the t-tests on range effects show no significant differences for the different combinations of lateral displacement instrument and altimeter. The t-test tests, however, did show a significant difference between the combinations of CDI and altimeter and HSI and altimeter at the 5 n. mi. range for standard deviation, but they showed no difference at 1.25 n. mi. and no difference in the mean at either range. The one significant difference that was noted can be attributed to the fact that the HSI and altimeter are located closer together on the instrument panel than are the CDI and altimeter; consequently, less scanning is required to read the HSI and altimeter combination.

With the ILS station, the glide slope indicators on the CDI and HSI instruments were used to display vertical error; therefore, a change in instrument sensitivity occurred with change in range. The t-tests applied to the data for each of these instruments show a significant change in standard deviation with range, but no significant differences in means. Comparison of the two instruments at each range shows that a significantly better standard deviation is obtained with the CDI than with the HSI at the 5 n. mi. range, but, as was the case with the lateral scores, no difference occurred at the 1.25 n. mi. range. The better CDI score results because the glide slope needle on the CDI is much longer than the needle on the HSI, and the motion of the needle is more visible; therefore, it provides a better indication of vertical error.

Pilot-Model Analysis

Lateral control.- To obtain a more detailed insight into pilot operations in lateral control with the CDI and HSI displays, a pilot-model matching exercise was carried out. For this analysis, some of the time histories obtained in the tests were matched through the use of a pilot model in the place of the pilot and through a trial-and-error adjustment of the pilot-model gains. The subjects chosen for matching (subjects MM, SH, and PB) represent low, medium, and high degrees of flight experience, respectively. Subject MM represented the low-performance, low-stability results, while subject PB provided some of the best results of the study.

The time history matches are shown in figures 10 to 14. The lateral displacement time histories are shown together with either the heading angle or bank angle time histories. The corresponding pilot-model matches are also shown together with the pilot-model gains required for each particular test. Runs which started with an initial lateral error but no wind are shown in figures 10 to 13, and runs with winds are shown in figure 14. Figure 10 indicates that when the displacement display sensitivity is low, i.e., at the 5 n. mi. range from the VOR station, the responses are characterized by a long-period, slow response that is well damped. As the display sensitivity is increased, the response becomes quicker, with shorter periods for the oscillatory mode, and not well damped. This trend is represented in the pilot model by increases in the outer-loop pilot-model gain K_y. With either the CDI or HSI, the pilot-

model gain increases with decrease in range. This result is true for the VOR station and, to a lesser extent, for the ILS station.

Closed-loop pilot-model-aircraft system characteristics were also determined and are shown in table VI. These system characteristics indicate an increase in the frequency of the roll-heading oscillatory mode corresponding to the increase in pilot-model gain K_y. For the tests made when tracking to the VOR station, this trend is clearly evident; the frequency of the roll-heading mode increases with the decrease in range, and the damping remains consistently high. These characteristics correspond to the improvement in system performance noted before.

It has already been noted that with the ILS station in use, the tracking accuracy did not improve with increase in display sensitivity. Model matching shows that the outer-loop gain K_y does increase with decrease in range, but that the inner-loop gains show a slight tendency toward a decrease. As a result of this tendency the system frequency does not change, and the system damping ratio shows a marked reduction. This decrease in system damping ratio corresponds to the lack of system performance improvement and represents a condition that could seriously affect flight safety.

The gain K_y represents the product of the instrument gain and the gain representing the pilot's response to the instrument. The instrument sensitivity changes by a factor of 10 between the conditions at 5 n. mi. from the VOR station and those at 1.25 n. mi. from the ILS station. Between these two conditions, the gain K_y changes by a factor of between 2 and 3. These values show that the pilot is attempting to adjust his gains to accommodate the change in instrument sensitivity but is not able to do so to the extent required to keep the system damping from falling to a low value.

The loss in system damping illustrated in the cases with no wind is further escalated by the addition of the wind. As shown in figure 14 and by the system characteristics shown in table VI (data for subject MM when using the ILS station), the system is stable at a range of 5 n. mi. but is unstable at a range of 1.25 n. mi. The data for subject MM with no winds show a reduction in system damping ratio from about 0.2 to 0.1.

A subjective judgment was made by the author on all the tests (20 for each condition) as to whether the system response was stable, neutrally stable, or divergent. Responses such as those shown in figure 13(b) for subject PB were judged stable; those for subject MM were called neutrally stable; and those for subject SH called divergent. It should be noted that the case for subject SH, which was called divergent, is shown by the pilot-model analysis to be stable, although with a low damping ratio. The results of these judgments are given in the following table:

Response	VOR				ILS			
	5 n. mi.		1.25 n. mi.		5 n. mi.		1.25 n. mi.	
	CDI	HSI	CDI	HSI	CDI	HSI	CDI	HSI
No wind								
Stable	18	19	18	16	18	18	12	17
Neutral	0	1	0	2	0	2	4	1
Divergent	2	0	2	2	2	0	4	2
With winds								
Stable	15	18	10	10	10	13	8	5
Neutral	2	2	2	6	5	4	3	5
Divergent	3	0	8	4	5	3	9	10

The preceding table shows the steady increase in the probability of very low system damping or outright instability that occurs with increase in display sensitivity as range is decreased.

In the fixed-base environment of the present tests, divergences occurred in a large percentage of the runs. These divergences resulted in part from the extended length of the runs (3 minutes), and from the fact that the subjects were asked to keep the error as low as they possibly could. In actual flight, the conditions that lead most often to divergence (the instrument sensitivity corresponding to a distance of 1.25 n. mi. from touchdown) would exist for a short time only. The pilot could be expected to be well stabilized on the desired path before reaching the 1.25 n. mi. range and to break out of the IFR conditions shortly thereafter. It is therefore unlikely that the fully developed divergences noted in the present tests would occur in a real IFR approach. However, the tests show that the potential for a pilot-induced unstable oscillation does exist with the present instrument systems. There is a small probability that as the aircraft approaches the middle marker, the pilot's attention could become completely occupied with the growing instability of the system. He could pass the decision height without notice and continue on toward the runway, with the display sensitivity continuing to increase. The system instability would continue to increase as the aircraft approached the ground. This situation could easily result in a crash.

The pilot-induced unstable oscillations encountered in the present tests do not have to persist once started. This is shown clearly in the sample test results presented in figure 15. In this particular case, a divergence starts and persists for 1-1/2 cycles. At that point, the pilot decided to stop responding to the lateral error. He concentrated fully on regulating the bank angle to 0°. During the period that he was stabilizing bank angle, a heading error of 5° existed. This heading error remained nearly constant for the 40 seconds that the pilot concentrated on bank angle. This constant heading

error led to a ramp change in lateral position which carried the aircraft from the right side of the desired path to the left side. At this point the pilot decided to resume control of displacement, which he did with an apparently well-damped response. The run was terminated before it became clear whether his second attempt at controlling displacement was successful.

Pilot-model analysis can also be used to provide a comparison between the COI and HSI. At the low sensitivity condition (5 n. mi. from the VOR), the pilot-model data show that a higher K_y gain is used with the HSI than with the CDI. Of even greater significance is the fact that the total pilot-model forward loop gain ($K^* = K_y K_\psi K_\phi$) is also higher for the HSI. As a result, the system roll-heading mode frequency is higher for the HSI, and for each instrument, the damping ratio is high and approximately equal. These results correspond to the better tracking accuracy obtained with the HSI. At the highest sensitivity (1.25 n. mi. from the ILS station), the system frequencies are nearly the same, and the damping ratios are low and nearly the same, results which correspond to the equal performance and the erratic time histories obtained with both instruments.

At a distance of 5 n. mi. from the ILS station, an anomaly appears in the pilot-model data: the performance measures show a significant difference between the two instruments, but the pilot-model data do not support this finding. In the case of the pilot-model data, mixed results are obtained; the pilot-model gain is higher for the HSI, but the system frequency for the HSI is lower. These results indicate that the performance with the two instruments should be about equal. The anomaly occurs because the three subjects chosen for the model-matching exercise obtained equal performance with the two instruments, as opposed to the results shown by the average of all 10 subjects, and it is this equal performance by the three subjects that is reflected in the pilot-model data.

As was mentioned in the section on statistical analysis of the performance data, a subjective judgment of the time histories obtained with the RMI indicates that the system performance with the RMI was considerably worse than that obtained with either the CDI or the HSI. Since the results with the RMI were so obvious, further analysis of the RMI data were not undertaken.

Vertical control.- Vertical control has less overall phase lag than does lateral control (one less integrator) and is easier to manage. Consequently, stable vertical control was obtained in all cases. Sample time histories of vertical control are shown in figure 8. A pilot-model analysis was not performed for vertical control.

CONCLUDING REMARKS

A six-degree-of-freedom, fixed-based simulation study of the use of conventional instruments in a general aviation Instrument Flight Rules (IFR) environment has been conducted. Ten subjects, who varied in flight experience from low-time student instrument pilots to professional test pilots, were used in the study. An important feature of the study was that the sensitivity of the displacement indicating instruments (the course deviation indicator (CDI),

the horizontal situation indicator (HSI), and the radio magnetic indicator (RMI)) was fixed at several different values to produce different test conditions.

A statistical analysis of performance for the path-following task showed that the accuracy of lateral path following improved with an increase in the sensitivity of the displacement indicating instruments up to the highest sensitivity. The maximum sensitivity tested corresponded to the sensitivity at 1.25 n. mi. from the glide slope station of an ILS system. The glide slope is 120 meters above the ground at this point. The tracking performance was no better at this point than it was at 5 n. mi. from the glide slope station.

Time history plots show that lateral displacement divergences occur in a high percentage of the tests conducted at the display sensitivity that exists at 1.25 n. mi. from the glide slope station. A pilot-model analysis confirms that the pilot-model-aircraft system exhibits adequate damping at low display sensitivity but near zero damping and even system instabilities at the highest test sensitivity. The low system damping results from the high pilot outer-loop gain used in conjunction with reduced inner-loop gains. These results indicate that a potentially unsafe flight condition exists when tracking the ILS signals at this distance from the station (1.25 n. mi. from the glide slope transmitter; 2.65 n. mi. from the localizer transmitter; or near the middle marker, typically).

These tests were also used to rank the effectiveness of the different instruments in promoting accurate path following. In the tests using the VOR station, the HSI provided the best lateral path-following accuracy, the CDI was second best, and the RMI was third. In tests with the ILS station, the HSI was better than the CDI at the 5 n. mi. range. Additionally, t-tests confirmed that these differences were significant at the 0.025 level. At the 1.25 n. mi. range, system damping dropped to low values with each of the two instruments, and performances were equal. The t-tests confirmed that there was no significant difference. In vertical control, the CDI performed better than the HSI at the condition of 5 n. mi. from the ILS station, again at the 0.025 significance level. At the 1.25 n. mi. range condition the performance of the two instruments were equal.

Langley Research Center
National Aeronautics and Space Administration
Hampton, VA 23665
November 26, 1980

REFERENCES

1. Forsyth, Donna L.; and Shaughnessy, John D.: Single Pilot IFR Operating Problems Determined From Accident Data Analysis. NASA TM-78773, 1978.

2. Smith, Ralph H.: A Theory for Longitudinal Short-Period Pilot Induced Oscillations. AFFDL-TR-77-57, U.S. Air Force, June 1977. (Available from DTIC as AD A056 982.)

3. Adams, James J.; and Hatch, Howard G., Jr.: An Approach to the Determination of Aircraft Handling Qualities by Using Pilot Transfer Functions. NASA TN D-6104, 1971.

4. Adams, James J.; and Moore, Frederick L.: An Analytical Study of Aircraft Lateral-Directional Handling Qualities Using Pilot Models. NASA TN D-8103, 1976.

TABLE I.- SAMPLE PILOT-MODEL-AIRCRAFT SYSTEM CHARACTERISTICS

(a) Complete system

Velocity, knots	Pilot-model gains			Closed-loop system characteristics							
				Control mode		Dutch roll mode		Roll-heading mode		y mode	
	K_ϕ	K_ψ	K_y, rad/m	ω_C, rad/sec	ζ_C	ω_{DR}, rad/sec	ζ_{DR}	ω_ϕ, rad/sec	ζ_ϕ	λ_1, sec-1	λ_2, sec-1
135	-0.16	1.25	0.00131	7.38	0.98	3.21	0.192	0.176	0.49	-0.206	-2.84
85	-.16	1.25	.00131	6.10	.97	1.99	.199	.226	.33	-.071	-2.87

(b) Successive loop closures

Velocity, knots	Pilot-model gains			Closed-loop system characteristics							
				Control mode		Dutch roll mode		Roll-heading mode			y mode
	K_ϕ	K_ψ	K_y, rad/m	ω_C, rad/sec	ζ_C	ω_{DR}, rad/sec	ζ_{DR}	ω_ϕ, rad/sec	ζ_ϕ	Real roots	
85	-0.16	1.25	0	6.10	0.97	1.99	0.198	0.25	0.43	λ_1 = 2.87	λ = 0
	-.16	0	0	6.13	.97	1.99	.202			λ_1 = -0.25 λ_2 = -2.81 λ_H = 0	λ = 0
	0	0	0			1.95	.208			λ_S = -0.023 λ_R = -4.94 λ_H = 0	λ = 0

TABLE II.- LATERAL STANDARD DEVIATIONS, IN METERS

(a) Scores, averages, and standard deviations of the scores

Subject	Day	VOR station						ILS station			
		5 n. mi.			1.25 n. mi.			5 n. mi.		1.25 n. mi.	
		RMI	CDI	HSI	RMI	CDI	HSI	CDI	HSI	CDI	HSI
DH	1		76.6	24.7		45.8	19.2	56.4	32.3	34.2	16.2
	2	61.6	55.5	13.1	60.1	17.1	23.8	23.2	24.1	16.2	14.6
MM	1		79.3	46.1		56.4	31.1	42.7	54.0	36.6	59.5
	2	68.9	52.5	36.3	205.9	36.9	26.2	54.6	45.1	111.9	125.7
JS	1		51.9	22.9		18.3	16.5	37.5	18.9	24.7	20.4
	2	31.4	55.5	31.7	50.6	20.4	19.2	37.5	34.5	43.0	24.1
JR	1		62.8	54.9		116.5	60.4	91.2	50.3	39.7	
	2	134.8	73.5	54.3	112.2	72.9	30.8	82.4	26.2	84.8	47.6
HV	1		50.3	20.7		31.7	29.9	39.7	38.1	29.0	28.1
	2	53.4	21.0	35.4	45.8	19.5	18.3	35.4	22.3	18.3	26.2
SS	1		133.9	39.3		63.4	24.4	68.3	42.7	31.1	47.9
	2	84.2	26.5	41.8	59.5	16.8	18.3	24.7	29.6	48.5	41.8
HB	1		55.2	21.4		16.2	15.3	29.3	25.6	38.7	26.8
	2	62.5	29.6	23.5	43.3	20.4	25.0	25.9	18.9	18.3	18.3
SH	1		23.8	25.0		19.5	16.2	35.7	34.2	32.6	32.0
	2	137.3	31.4	25.9	95.5	21.4	15.3	18.9	25.6	69.2	20.7
PB	1		44.8	14.0		15.3	10.1	27.1	21.4	25.0	27.1
	2		37.8	24.1		23.8	14.9	19.5	12.8	14.0	
PD	1		43.6	42.4		37.8	22.0	27.5	30.5	35.4	18.6
	2		53.7	26.5		33.2	15.6	51.2	13.1	15.3	18.6
Average		79.26	52.96	31.20	84.11	35.17	22.63	41.44	30.01	38.33	34.12
Standard deviation		38.06	25.46	12.15	55.01	25.52	10.65	20.34	11.55	24.74	26.09

TABLE II.- Concluded

(b) Results for t-test on lateral standard deviation comparisons

Range effects

Conditions	P-value
VOR station	
RMI: 5 n. mi. to 1.25 n. mi.	0.40
CDI: 5 n. mi. to 1.25 n. mi.	.005
HSI: 5 n. mi. to 1.25 n. mi.	.0005
ILS station	
CDI: 5 n. mi. to 1.25 n. mi.	>0.40
HSI: 5 n. mi. to 1.25 n. mi.	>.40

Display effects

Conditions		P-value
VOR station		
5 n. mi.:	CDI - HSI	0.0005
	CDI - RMI	.025
	HSI - RMI	.005
1.25 n. mi.:	CDI - HSI	.005
	CDI - RMI	.010
	HSI - RMI	.010
ILS station		
5 n. mi.:	CDI - HSI	0.005
1.25 n. mi.:	CDI - HSI	.20

TABLE III.- LATERAL MEANS, IN METERS

(a) Scores, averages, and standard deviations of the scores

Subject	Day	VOR station						ILS station			
		5 n. mi.			1.25 n. mi.			5 n. mi.		1.25 n. mi.	
		RMI	CDI	HSI	RMI	CDI	HSI	CDI	HSI	CDI	HSI
DH	1		30.8	-50.3		-3.4	-31.7	56.7	-15.9	22.0	-3.4
	2	98.5	32.9	12.2	102.8	20.4	7.8	-3.7	18.0	20.1	10.4
MM	1		88.1	-5.2		16.2	11.9	24.1	15.9	38.4	59.5
	2	123.5	53.0	-11.6	170.5	3.1	-7.6	39.0	34.2	130.2	117.1
JS	1		60.4	9.8		6.4	3.1	22.9	7.6	26.8	-2.1
	2	8.8	90.9	11.6	43.3	10.1	-11.9	-12.8	-15.6	-3.7	7.0
JR	1		-88.8	-83.6		-3.1	-6.1	-20.4	29.6	-30.5	
	2	79.9	180.9	99.7	70.8	14.0	17.1	4.6	3.4	-34.8	0.92
HV	1		20.4	-36.6		-12.2	-15.6	10.7	7.3	13.7	1.83
	2	60.4	16.2	9.2	63.1	-11.0	-3.7	33.2	9.5	14.9	22.6
SS	1		-89.1	1.53		-22.3	2.44	54.0	3.05	-7.32	6.10
	2	56.4	61.6	2.44	60.7	11.9	3.05	25.9	9.15	-4.27	18.3
HB	1		54.3	11.3		7.93	11.9	56.1	48.8	34.8	22.3
	2	127.5	52.8	18.3	12.5	-3.05	13.1	28.7	29.9	7.93	10.1
SH	1		68.6	34.8		19.8	8.85	40.0	19.2	33.2	-3.66
	2	164.7	39.0	46.4	-12.2	-5.5	22.8	26.2	12.5	37.8	8.85
PB	1		133.3	8.24		44.8	-1.5	43.3	21.4	16.5	4.0
	2		76.3	7.63		10.7	10.9	19.8	12.5	13.7	
PD	1		98.8	85.1		18.9	19.5	60.7	30.8	31.4	10.7
	2		98.5	66.2		-22.3	17.1	20.4	29.6	19.5	19.2
Average		89.96	53.95	11.86	63.94	5.07	3.03	26.47	15.55	19.02	17.21
Standard deviation		49.11	62.56	42.43	55.80	16.01	13.40	22.79	15.95	33.30	28.87

TABLE III.- Concluded

(b) *Results for t-test on lateral means comparisons*

Range effects

Conditions	P-value
VOR station	
RMI: 5 n. mi. to 1.25 n. mi.	0.20
CDI: 5 n. mi. to 1.25 n. mi.	.0005
HSI: 5 n. mi. to 1.25 n. mi.	.20
ILS station	
CDI: 5 n. mi. to 1.25 n. mi.	0.20
HSI: 5 n. mi. to 1.25 n. mi.	.40

Display effects

Conditions		P-value
VOR station		
5 n. mi.:	CDI - HSI	0.0005
	CDI - RMI	>.40
	HSI - RMI	.005
1.25 n. mi.:	CDI - HSI	.40
	CDI - RMI	.01
	HSI - RMI	.025
ILS station		
5 n. mi.:	CDI - HSI	0.05
1.25 n. mi.:	CDI - HSI	.20

TABLE IV.- VERTICAL STANDARD DEVIATION, IN METERS

(a) Scores, averages, and standard deviations of the scores

Subject	Day	VOR station						ILS station			
		5 n. mi.			1.25 n. mi.			5 n. mi.		1.25 n. mi.	
		RMI	CDI	HSI	RMI	CDI	HSI	CDI	HSI	CDI	HSI
DH	1		10.10	2.53		7.20	3.78	10.80	13.88	6.83	5.03
	2	3.63	8.42	6.74	8.57	5.52	3.57	11.13	12.44	6.74	9.91
MM	1		18.76	7.81		6.80	7.26	11.53	15.59	7.81	10.07
	2	13.18	6.34	5.64	37.52	14.18	11.96	7.14	8.88	9.52	20.53
JS	1		6.53	5.34		5.37	5.95	20.01	15.16	6.74	8.75
	2	5.73	6.59	4.73	9.67	4.61	6.16	9.39	13.30	7.78	9.58
JR	1		6.38	11.90		10.92	7.17	7.84	16.78	6.38	
	2	11.07	19.89	7.08	11.83	6.19	10.10	7.60	17.20	12.75	9.09
HV	1		6.01	4.18		8.54	5.86	11.65	13.05	5.64	6.47
	2	5.73	5.64	5.86	5.98	4.79	3.20	6.13	9.03	3.94	7.47
SS	1		5.58	7.53		6.47	8.02	8.14	13.24	7.69	8.05
	2	21.32	11.19	9.21	11.29	32.54	12.02	13.45	14.67	6.68	11.07
HB	1		7.75	4.30		3.36	4.30	6.53	8.39	5.92	6.07
	2	13.42	5.95	5.06	8.17	6.62	5.16	10.65	13.39	10.58	12.78
SH	1		6.10	4.94		7.11	5.86	10.58	9.61	7.69	8.39
	2	7.05	4.76	6.22	6.07	3.42	6.62	7.08	9.61	8.60	6.44
PB	1		9.15	3.90		7.38	5.00	6.44	18.42	5.64	
	2		2.99	2.53		4.45	3.78	7.41	6.41	5.64	5.70
PD	1		15.77	5.09		5.73	4.09	5.46	6.44	4.73	4.88
	2		6.01	5.09		9.12	7.20	12.63	3.48	10.71	5.86
Average		10.14	8.50	5.74	12.39	8.02	6.35	9.58	11.95	7.40	8.67
Standard deviation		5.21	4.59	2.20	10.37	6.30	2.58	3.41	4.03	2.17	3.68

TABLE IV.- Concluded

(b) Results for t-test on vertical standard deviation comparisons

Range effects

Conditions	P-value
VOR station	
RMI: 5 n. mi. to 1.25 n. mi.	0.30
CDI: 5 n. mi. to 1.25 n. mi.	.40
HSI: 5 n. mi. to 1.25 n. mi.	.20
ILS station	
CDI: 5 n. mi. to 1.25 n. mi.	0.01
HSI: 5 n. mi. to 1.25 n. mi.	.01

Display effects

Conditions		P-value
VOR station		
5 n. mi.:	CDI - HSI	0.01
	CDI - RMI	.30
	HSI - RMI	.05
1.25 n. mi.:	CDI - HSI	.10
	CDI - RMI	.30
	HSI - RMI	.10
ILS station		
5 n. mi.:	CDI - HSI	0.025
1.25 n. mi.:	CDI - HSI	.10

TABLE V.- VERTICAL MEANS, IN METERS

(a) Scores, averages, and standard deviations of the scores

Subject	Day	VOR station						ILS station			
		5 n. mi.			1.25 n. mi.			5 n. mi.		1.25 n. mi.	
		RMI	CDI	HSI	RMI	CDI	HSI	CDI	HSI	CDI	HSI
DH	1		-2.75	-5.31		0.43	-7.11	-2.38	-5.37	-1.89	0.70
	2	-0.95	-2.35	-3.57	11.65	4.30	.88	14.21	-5.34	-2.65	-3.51
MM	1		9.91	4.58		7.72	-14.98	-13.66	10.71	-4.73	2.96
	2	24.07	-1.22	-1.17	-16.10	-8.08	-7.66	-18.21	14.06	-8.72	-17.78
JS	1		-6.25	-4.27		-3.48	-9.49	1.74	9.61	-4.15	-1.28
	2	-1.98	-9.36	-1.92	5.58	-6.92	-2.78	27.69	.85	-2.14	-.64
JR	1		-3.51	8.75		10.77	-2.20	0.46	27.21	-15.34	
	2	12.96	1.10	12.69	9.73	-6.13	6.47	-21.96	-2.72	-.31	-12.66
HV	1		-4.67	0.55		-3.90	1.86	-0.46	4.61	-5.98	-0.92
	2	-3.20	-10.58	1.31	0.21	-2.87	-2.84	-5.73	16.23	-4.82	.49
SS	1		5.89	4.73		-4.12	-1.56	4.79	8.33	-4.70	-1.71
	2	35.08	20.31	-3.23	13.18	72.29	-1.16	-33.52	-39.41	-16.23	-9.09
HB	1		-2.72	-2.41		5.28	0.55	-0.49	-18.79	-5.52	-9.55
	2	-19.15	-8.30	-5.61	-3.29	-5.64	3.05	-11.47	-17.69	-7.81	4.79
SH	1		-4.51	-6.99		-8.54	-5.19	2.56	-16.10	-1.34	0.52
	2	-7.99	-6.44	-9.97	-10.13	-5.77	-7.99	1.34	-13.24	-7.90	-2.01
PB	1		3.33	-0.92		4.36	2.81	-4.61	-17.97	-2.90	
	2		-8.39	-6.99		-4.48	-7.50	1.74	.55	-4.48	0.89
PD	1		-16.99	-8.45		-0.67	-0.61	-3.05	4.67	-1.68	0.37
	2		1.01	-1.89		-14.12	4.39	12.26	-9.82	-2.26	.09
Average		4.86	-2.32	-2.04	1.35	1.52	-2.55	-2.44	-2.48	-5.28	-2.69
Standard deviation		17.86	8.06	5.72	10.64	17.74	5.37	13.30	15.45	4.26	5.22

TABLE V.- Concluded

(b) Results for t-test on vertical means comparisons

Range effects

Conditions	P-value
VOR station	
RMI: 5 n. mi. to 1.25 n. mi.	0.40
CDI: 5 n. mi. to 1.25 n. mi.	.20
HSI: 5 n. mi. to 1.25 n. mi.	.40
ILS station	
CDI: 5 n. mi. to 1.25 n. mi.	0.20
HSI: 5 n. mi. to 1.25 n. mi.	>.40

Display effects

Conditions		P-value
VOR station		
5 n. mi.:	CDI - HSI	0.41
	CDI - RMI	.20
	HSI - RMI	.20
1.25 n. mi.:	CDI - HSI	.40
	CDI - RMI	.40
	HSI - RMI	.05
ILS station		
5 n. mi.:	CDI - HSI	<0.40
1.25 n. mi.:	CDI - HSI	.01

TABLE VI.- PILOT-MODEL-AIRCRAFT SYSTEM CHARACTERISTICS

(a) VOR station

Subject	Pilot-model gains			Closed loop system characteristics							
				Control mode		Dutch roll mode		Roll-heading mode		y-mode	
	K_ϕ	K_ψ	K_y, rad/m	ω_C, rad/sec	ζ_C	ω_{DR}, rad/sec	ζ_{DR}	ω_ϕ, rad/sec	ζ_ϕ	λ_1, sec^{-1}	λ_2, sec^{-1}
5 n. mi. from VOR station, CDI											
MM	-0.24	0.67	0.00131	7.63	0.97	3.21	0.186	0.100	0.44	-0.611	-2.20
SH	-.24	.63	.00082	7.61	.97	3.22	.186	.077	.59	-.611	-2.20
PB	-.34	1.33	.00082	7.61	.98	3.21	.186	.157	1.07	-.303	-2.28
Average			.00098					.111			
5 n. mi. from VOR station, HSI											
MM	-0.12	1.0	0.00108	7.25	0.99	3.18	0.194	0.137	0.45	-0.157	-3.13
SH	-.12	1.0	.00108	7.25	.99	3.18	.194	.137	.45	-.157	-3.13
PB	-.24	1.33	.00164	7.61	.98	3.21	.186	.183	.54	-.443	-2.27
Average			.00128					.152			
1.25 n. mi. from VOR station, CDI											
MM	-0.24	1.33	0.00246	7.60	0.98	3.21	0.186	0.211	0.340	-0.500	-2.27
SH	-.24	.67	.00164	7.60	.98	3.21	.186	.111	.368	-.618	-2.20
PB	-.32	1.25	.00197	7.79	.99	3.23	.179	.178	.49	-1.00	-1.50
Average			.00203					.166			
1.25 n. mi. from VOR station, HSI											
MM	-0.24	1.33	0.00246	7.60	0.98	3.21	0.186	0.211	0.34	-0.500	-2.27
SH	-.24	1.33	.00206	7.63	.97	3.21	.186	.199	.42	-.476	-2.27
PB	-.16	2.50	.00164	7.40	.98	3.19	.191	.318	.288	-.155	-2.91
Average			.00208					.243			

TABLE VI.- Continued

(b) ILS station

Subject	Pilot-model gains			Closed-loop system characteristics							
				Control mode		Dutch roll mode		Roll-heading mode		y-mode	
	K_ϕ	K_ψ	K_y, rad/m	ω_C, rad/sec	ζ_C	ω_{DR}, rad/sec	ζ_{DR}	ω_ϕ, rad/sec	ζ_ϕ	λ_1, sec^{-1}	λ_2, sec^{-1}
5 n. mi. from ILS station, CDI											
MM	-0.16	1.50	0.00219	6.10	0.97	1.99	0.198	0.245	0.185	-0.118	-2.89
SH	-.16	1.50	.00164	6.10	.97	1.99	.198	.248	.248	-.087	-2.89
PB	-.16	1.50	.00164	6.10	.97	1.99	.198	.248	.248	-.087	-2.89
Average			.00183					.247			
5 n. mi. from ILS station, HSI											
MM	-0.16	1.0	0.00246	6.10	0.97	1.99	0.199	0.190	0.199	-0.149	-2.85
SH	-.16	1.0	.00164	6.10	.97	1.99	.200	.189	.33	-.099	-2.85
PB	-.24	1.67	.00262	6.30	.96	2.01	.193	.315	.254	-.151	-2.56
Average			.00217					.231			
1.25 n. mi. from ILS station, CDI											
MM	-0.16	1.0	0.00328	6.10	0.97	1.99	0.200	0.297	0.104	-0.184	-2.85
SH	-.16	1.50	.00272	6.10	.97	1.99	.198	.245	.130	-.146	-2.89
PB	-.16	1.50	.00220	6.10	.97	1.99	.198	.246	.187	-.118	-2.89
Average			.00278					.229			
1.25 n. mi. from VOR station, HSI											
MM	-0.16	1.50	0.00272	6.10	0.97	2.00	0.198	0.248	0.130	-0.146	-2.89
SH	-.16	.75	.00425	6.10	.97	1.99	.200	.178	.031	-.221	-2.84
PB	-.16	1.00	.00272	6.30	.98	2.02	.196	.216	.322	-.204	-2.46
Average			.00326					.213			

TABLE VI.- Concluded

(c) ILS station with winds

Subject	Pilot-model gains			Closed loop system characteristics							
				Control mode		Dutch roll mode		Roll-heading mode		y-mode	
	K_ϕ	K_ψ	K_y, rad/m	ω_C, rad/sec	ζ_C	ω_{DR}, rad/sec	ζ_{DR}	ω_ϕ, rad/sec	ζ_ϕ	λ_1, sec^{-1}	λ_2, sec^{-1}
5 n. mi. from ILS station, CDI with winds											
MM	-0.16	2.00	0.00202	6.10	0.97	2.00	0.198	0.291	0.159	-0.103	-2.93
5 n. mi. from ILS station, HSI with winds											
MM	-0.24	1.33	0.00082	6.30	0.96	2.02	0.194	0.305	0.461	-0.410	-2.50
1.25 n. mi. from ILS station, HSI with winds											
MM	-0.04	3.00	0.00272	5.64	0.99	1.96	0.205	0.195	-0.128	-0.108	-3.79
1.25 n. mi. from ILS station, CDI with winds											
MM	-0.08	1.50	0.00425	5.85	0.98	1.97	0.202	0.201	-0.125	-0.165	-3.38

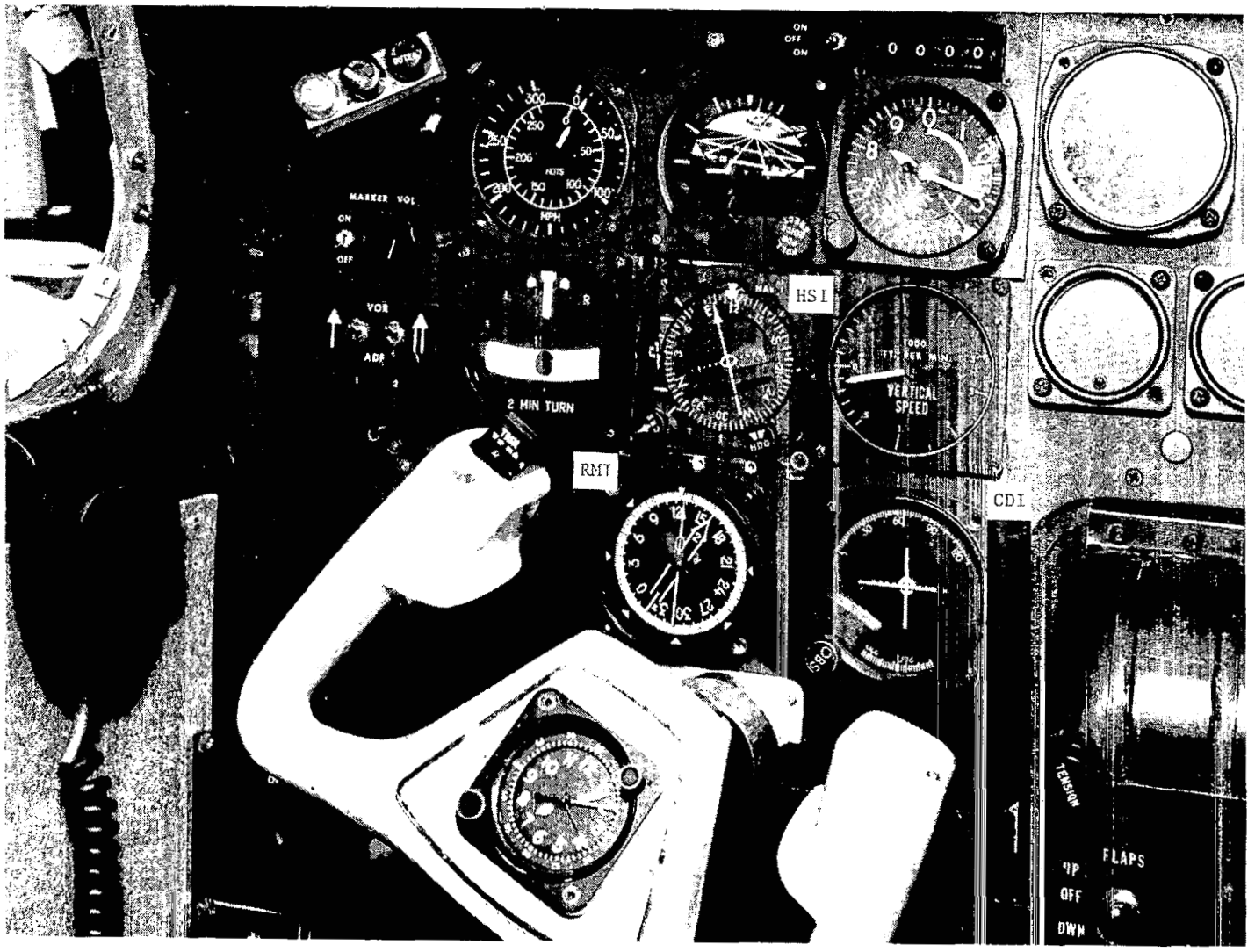

L-80-2370

Figure 1.- Simulator display panel.

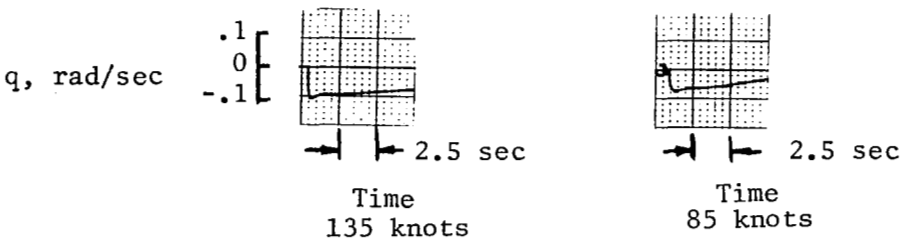

(a) Short-period longitudinal response to a 0.02-rad elevator step.

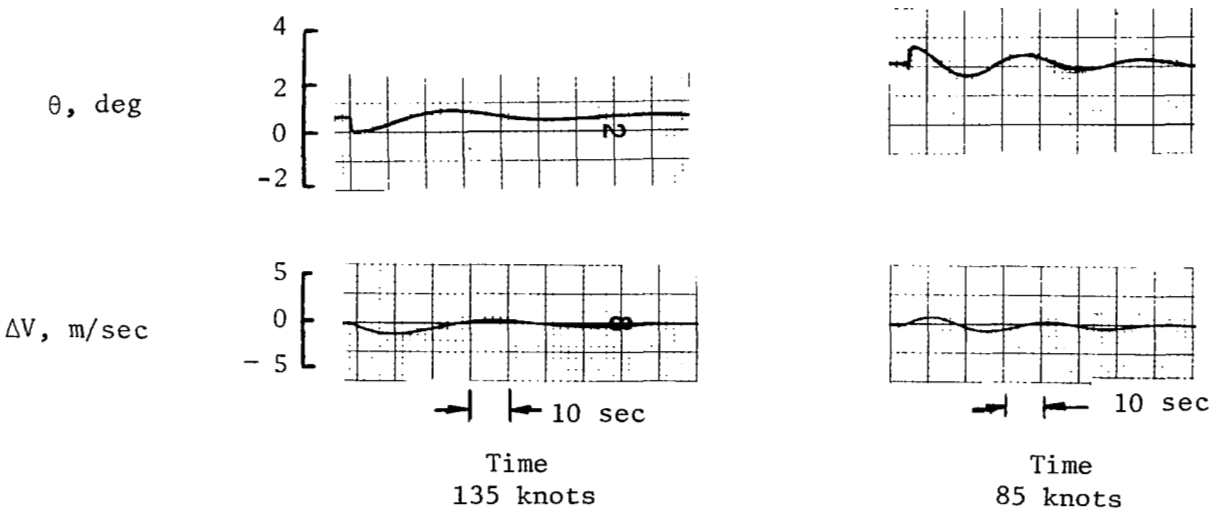

(b) Phugoid response to an initial out-of-trim α.

Figure 2.- Longitudinal response of aircraft.

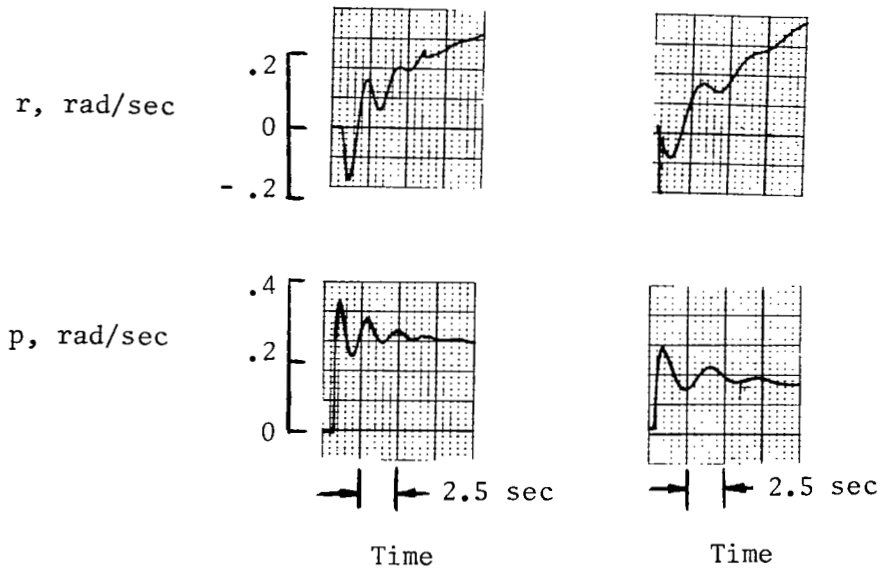

(a) 135 knots. (b) 85 knots.

Figure 3.- Lateral response to a 0.068-rad aileron step.

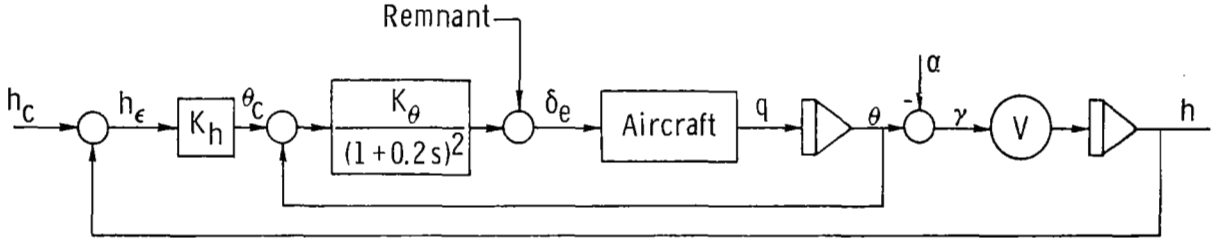

(a) Longitudinal system.

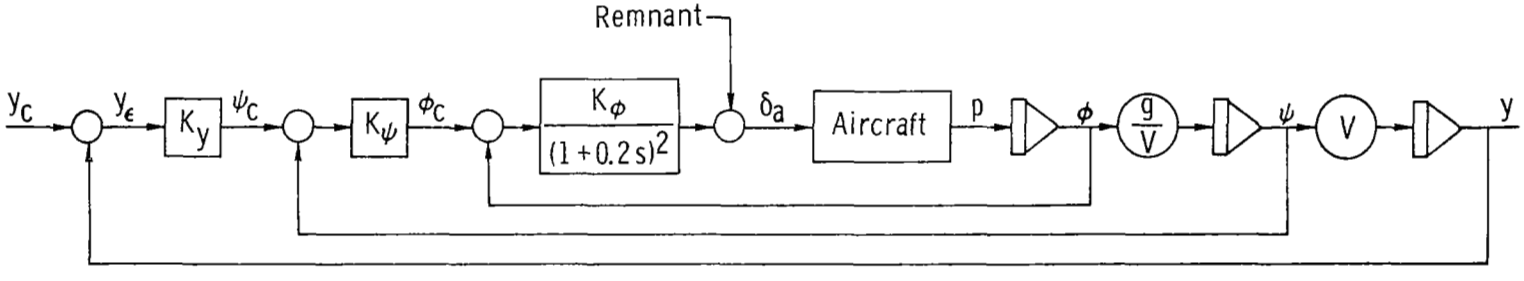

(b) Lateral system.

Figure 4.- Pilot-model-aircraft system.

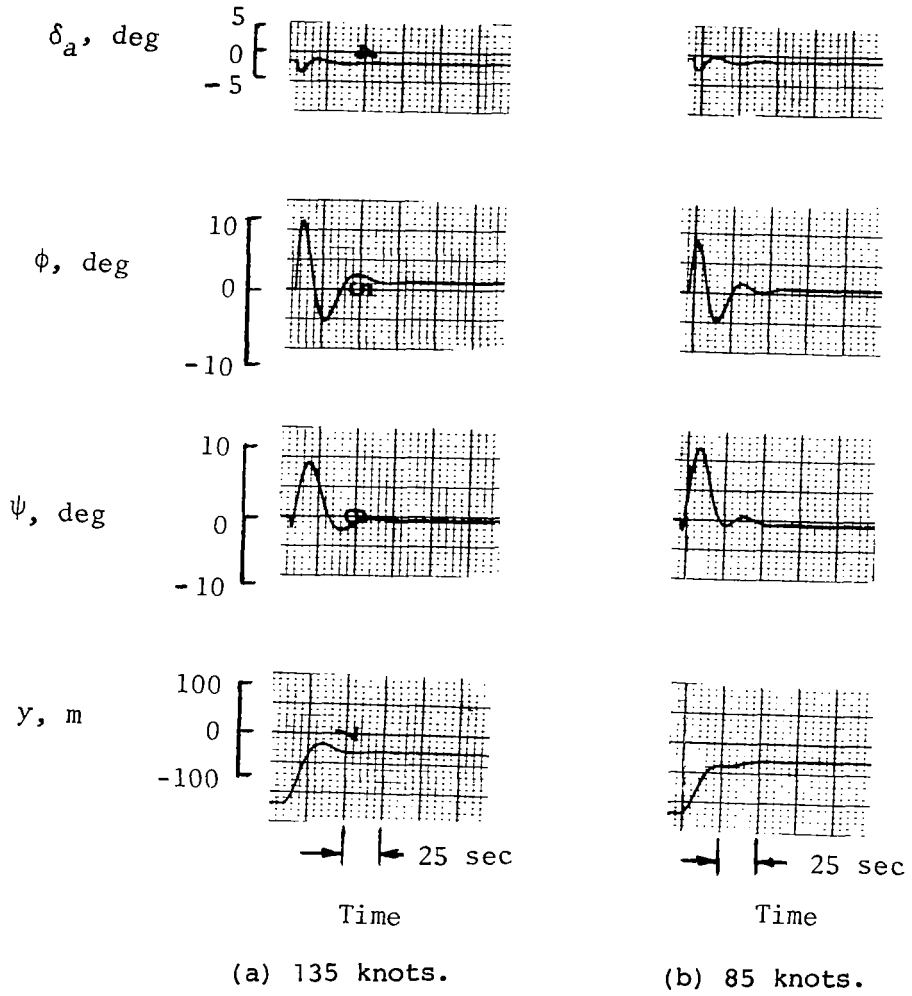

(a) 135 knots. (b) 85 knots.

Figure 5.- Pilot-model plus aircraft response. $K_\phi = -0.16$; $K_\psi = 1.25$; $K_y = 0.00131$ rad/m.

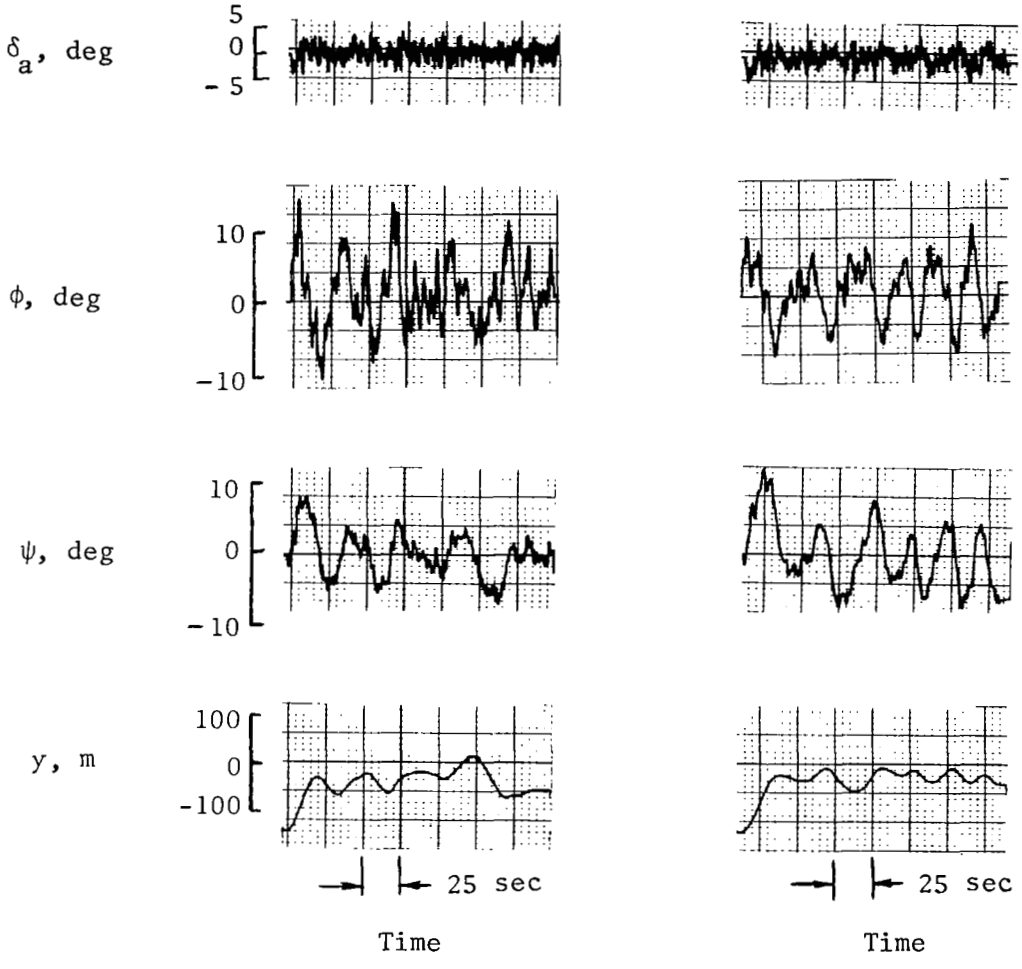

(a) 135 knots.

(b) 85 knots.

Figure 6.- Pilot-model plus aircraft response with pilot remnant. $K_\phi = -0.16$; $K_\psi = 1.25$; $K_y = 0.00131$ rad/m.

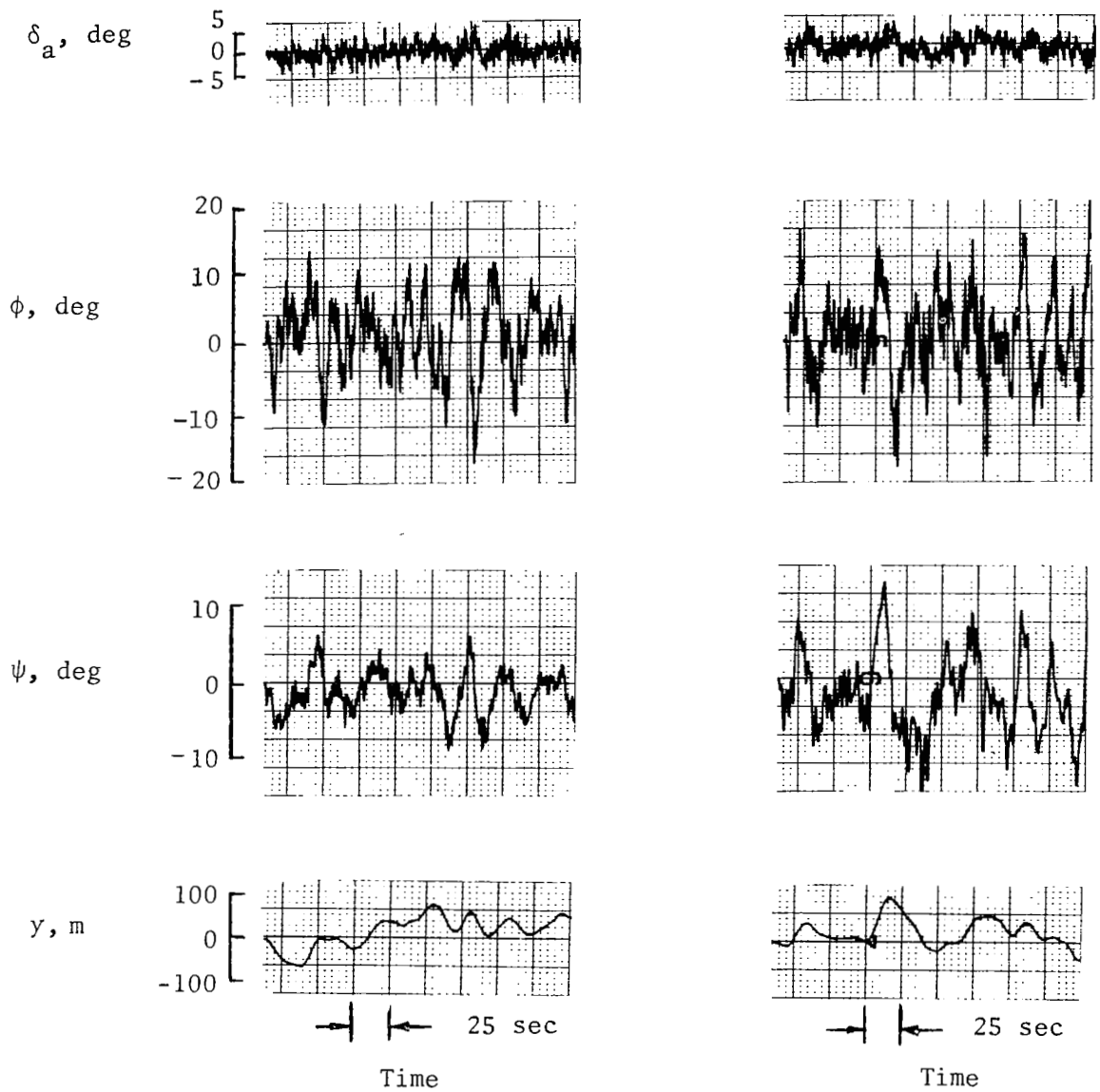

(a) 135 knots. (b) 85 knots.

Figure 7.- Pilot-model plus aircraft response with wind disturbance. $K_\phi = -0.16$; $K_\psi = 1.25$; $K_y = 0.00131$ rad/m.

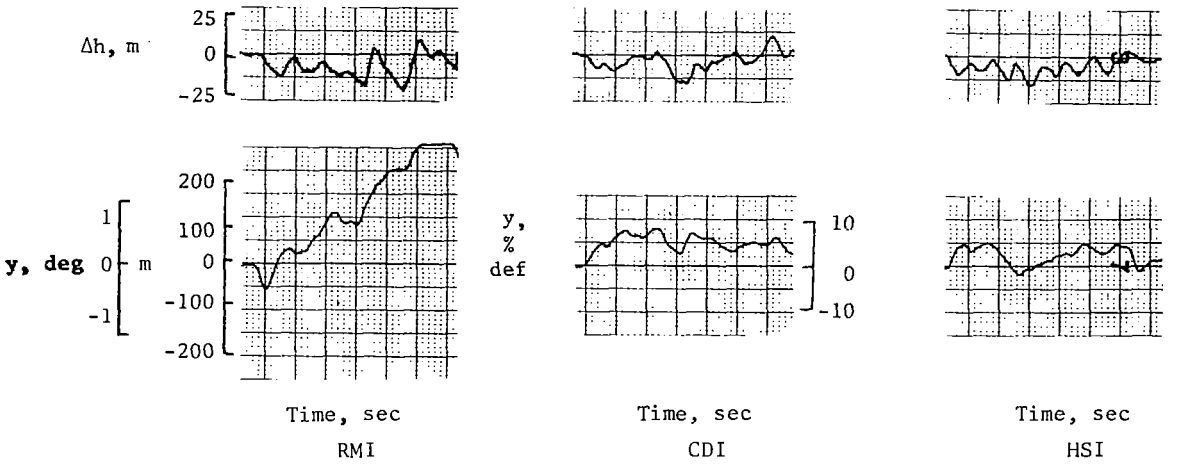

(a) VOR, 5 n. mi.

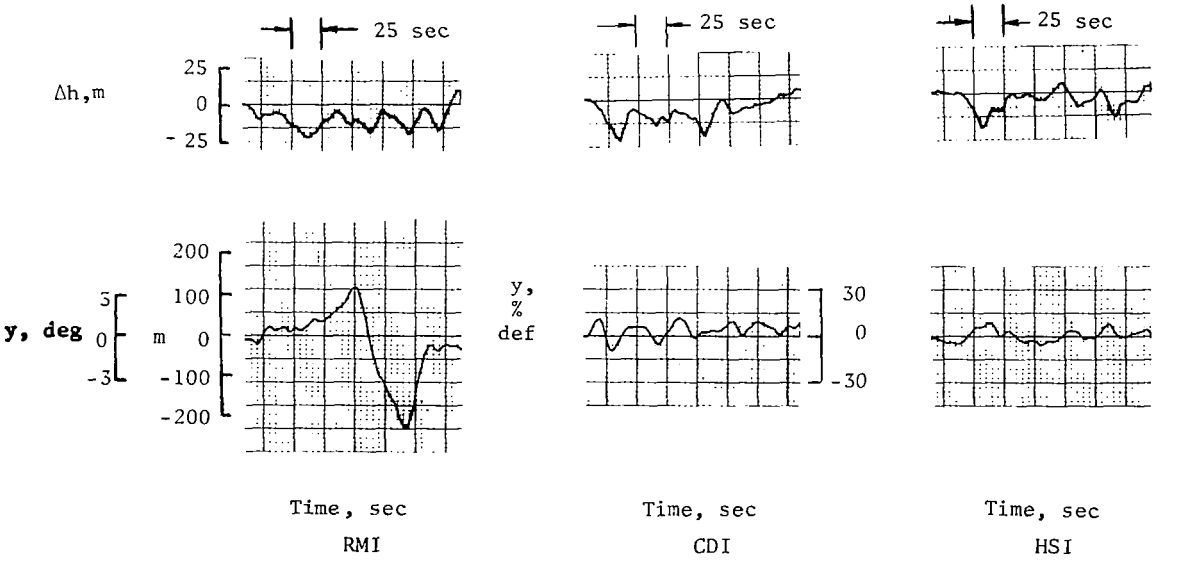

(b) VOR, 1.25 n. mi.

Figure 8.- Sample time histories with winds for subject SH.

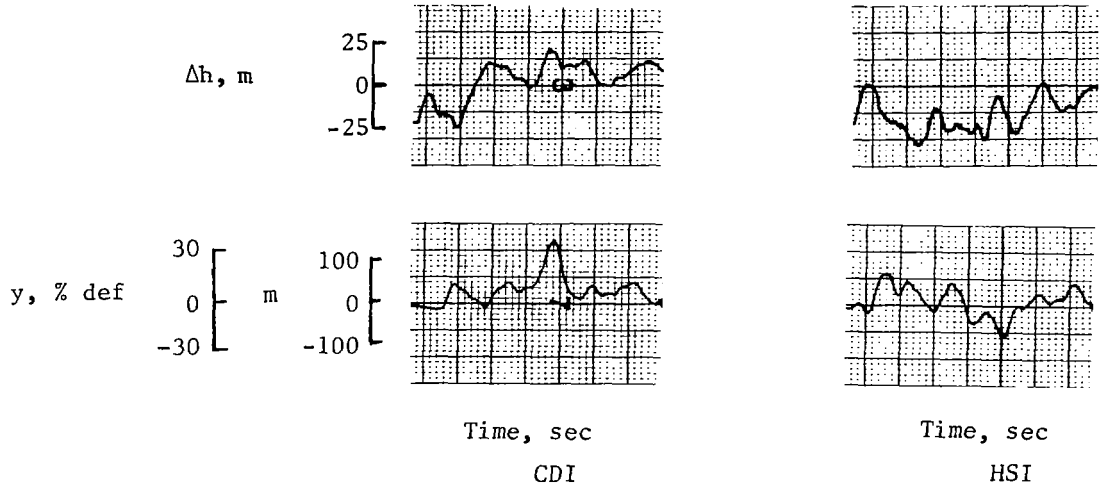

(c) ILS, 5 n. mi.

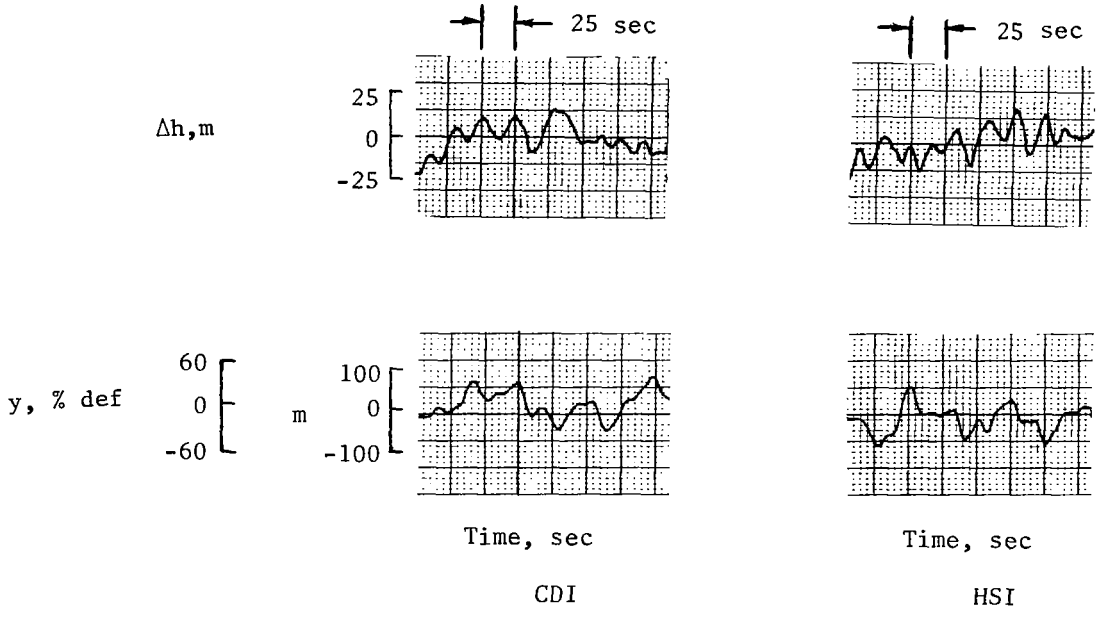

(d) ILS, 1.25 n. mi.

Figure 8.- Concluded.

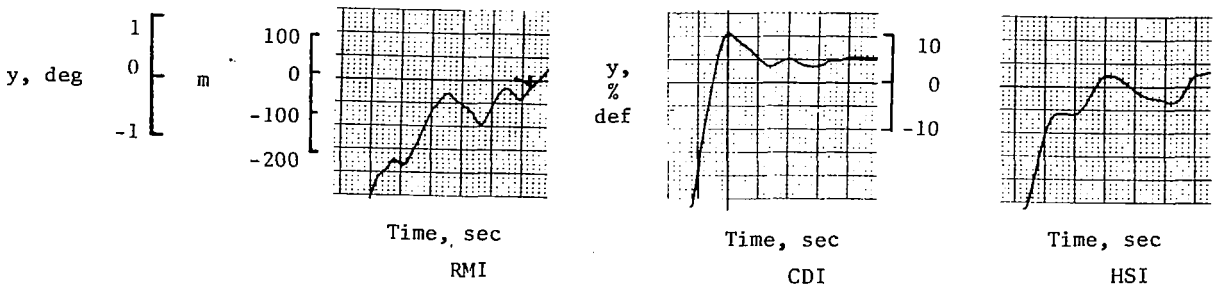

(a) VOR, 5 n. mi.

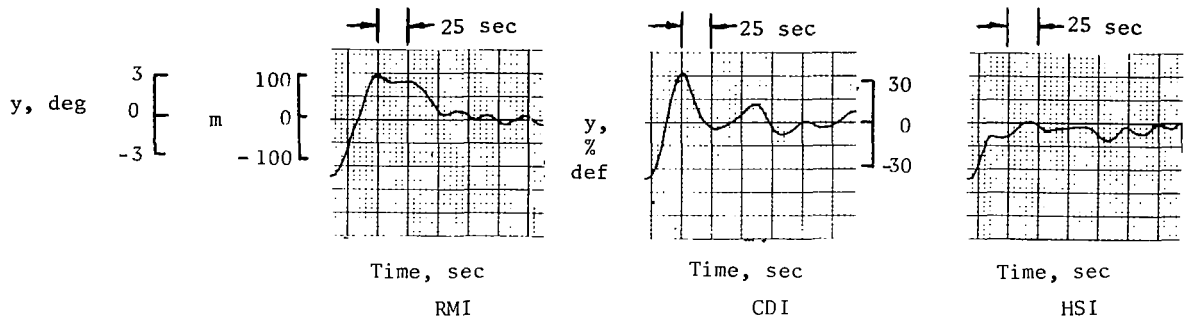

(b) VOR, 1.25 n. mi.

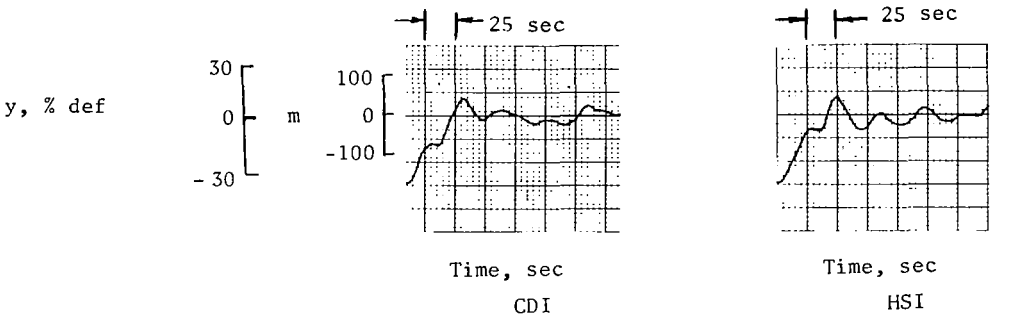

(c) ILS, 5 n. mi.

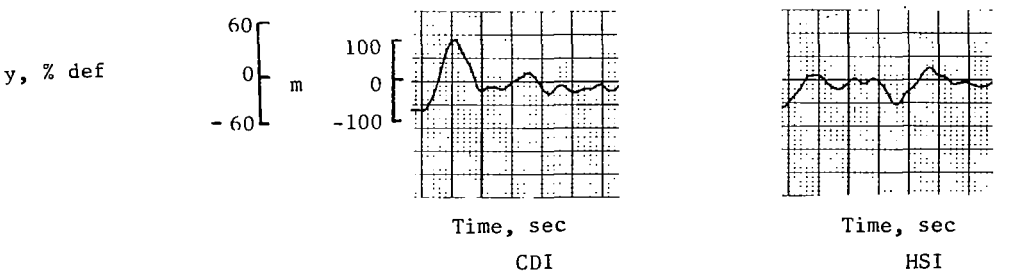

(d) ILS, 1.25 n. mi.

Figure 9.- Sample time histories with initial error, no winds for subject SH.

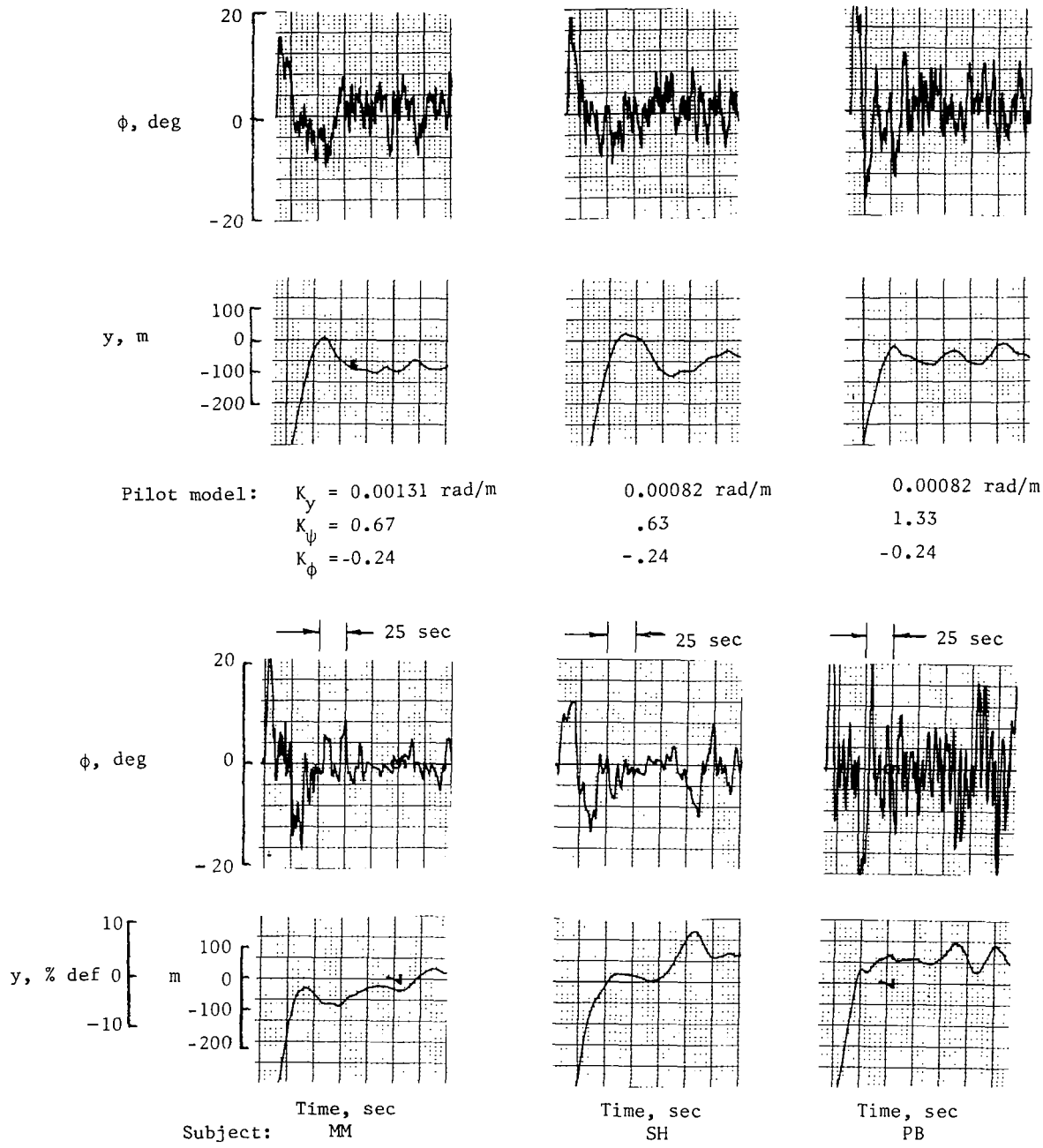

(a) CDI.

Figure 10.- Responses with VOR station at 5 n. mi. range.

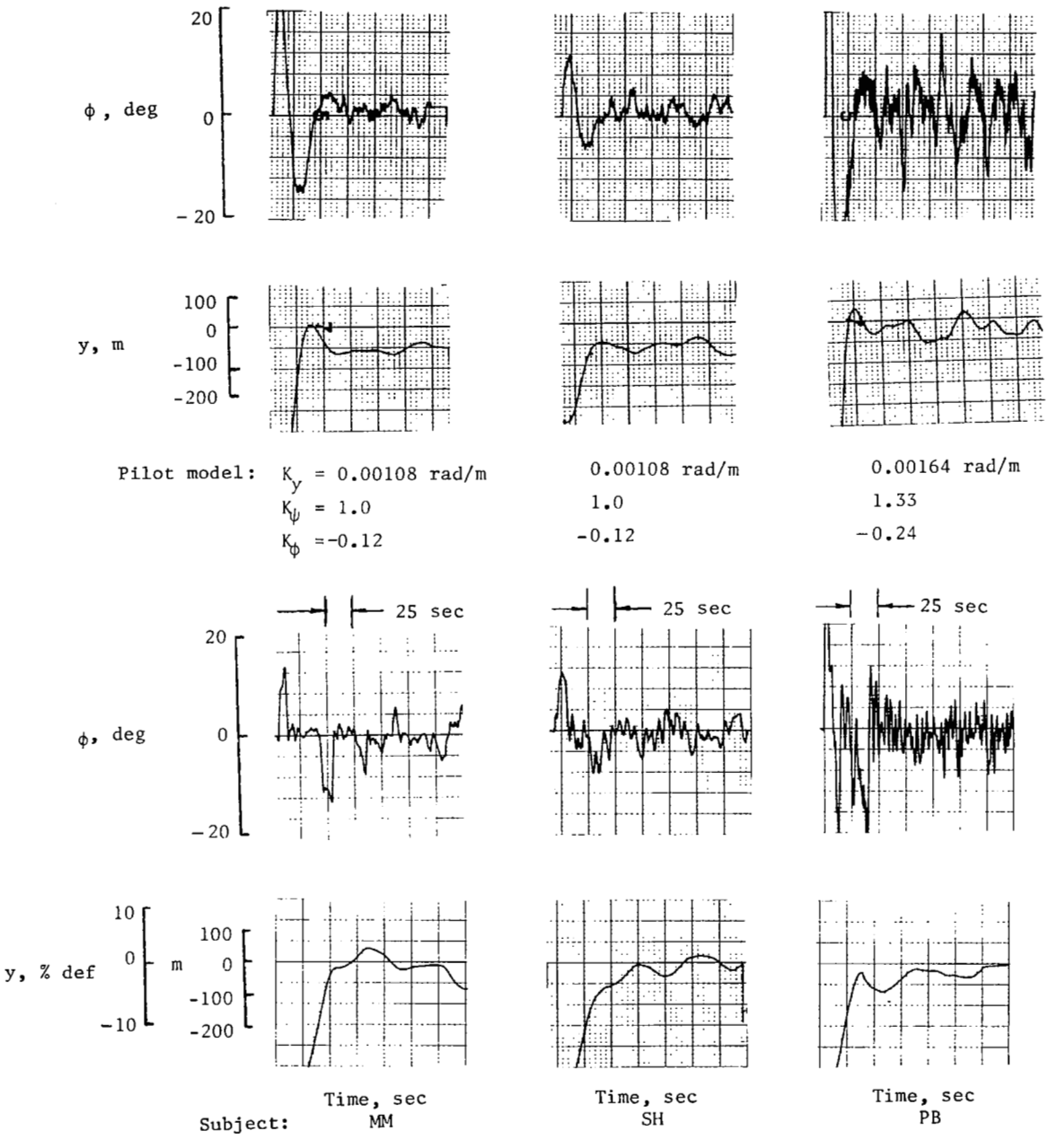

(b) HSI.

Figure 10.- Concluded.

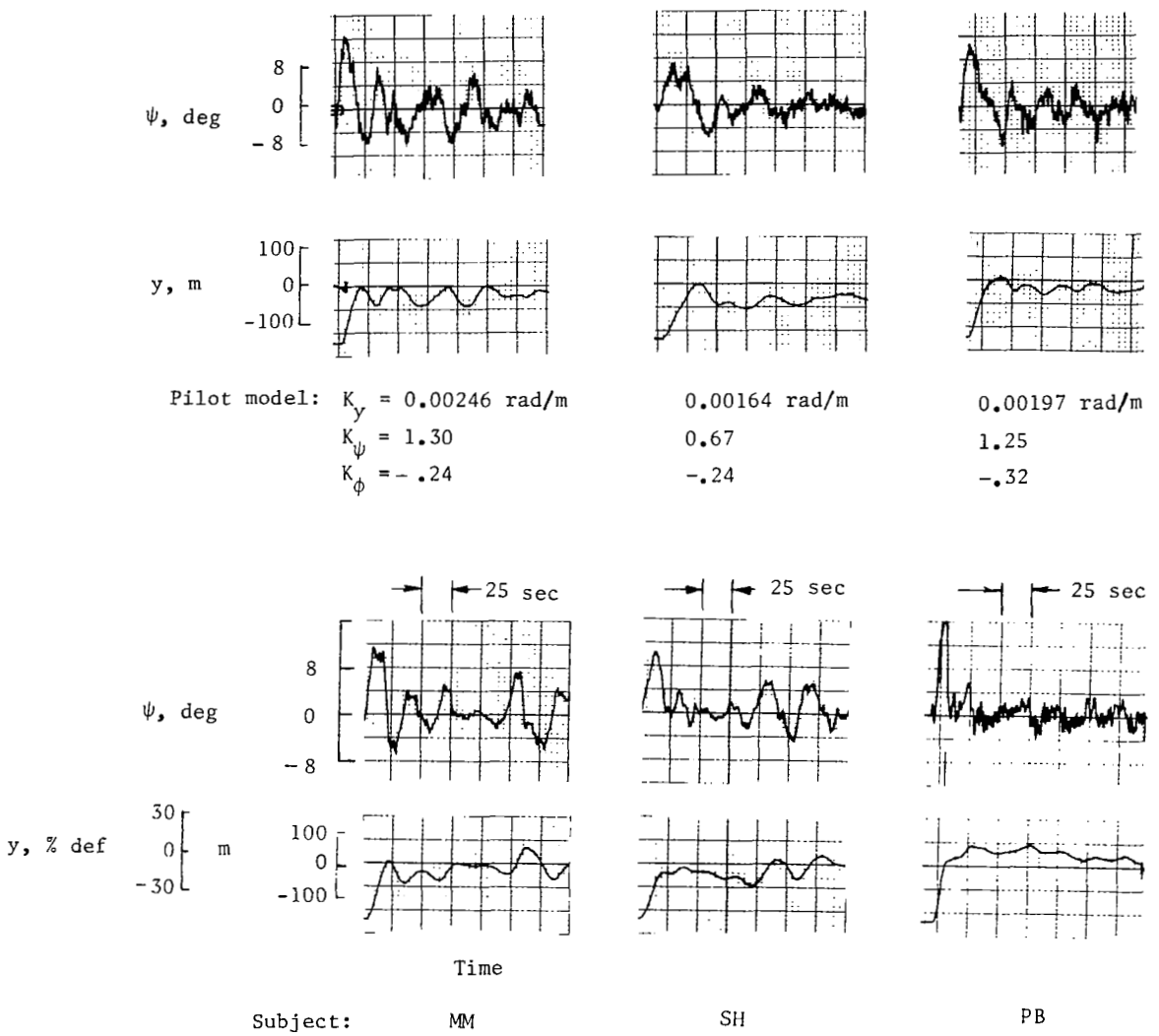

(a) CDI.

Figure 11.- Responses with VOR station at 1.25 n. mi. range.

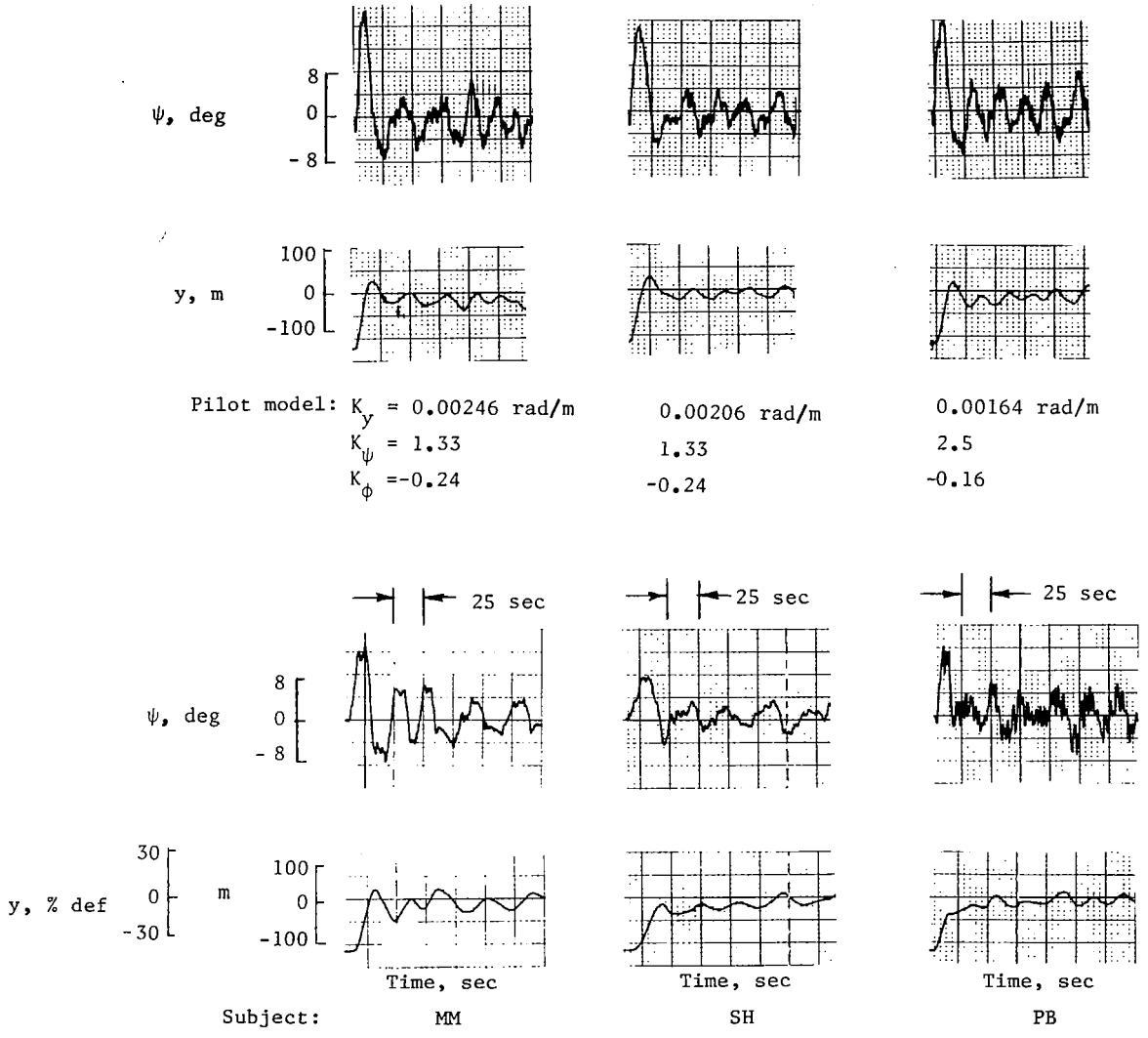

(b) HSI.

Figure 11.- Concluded.

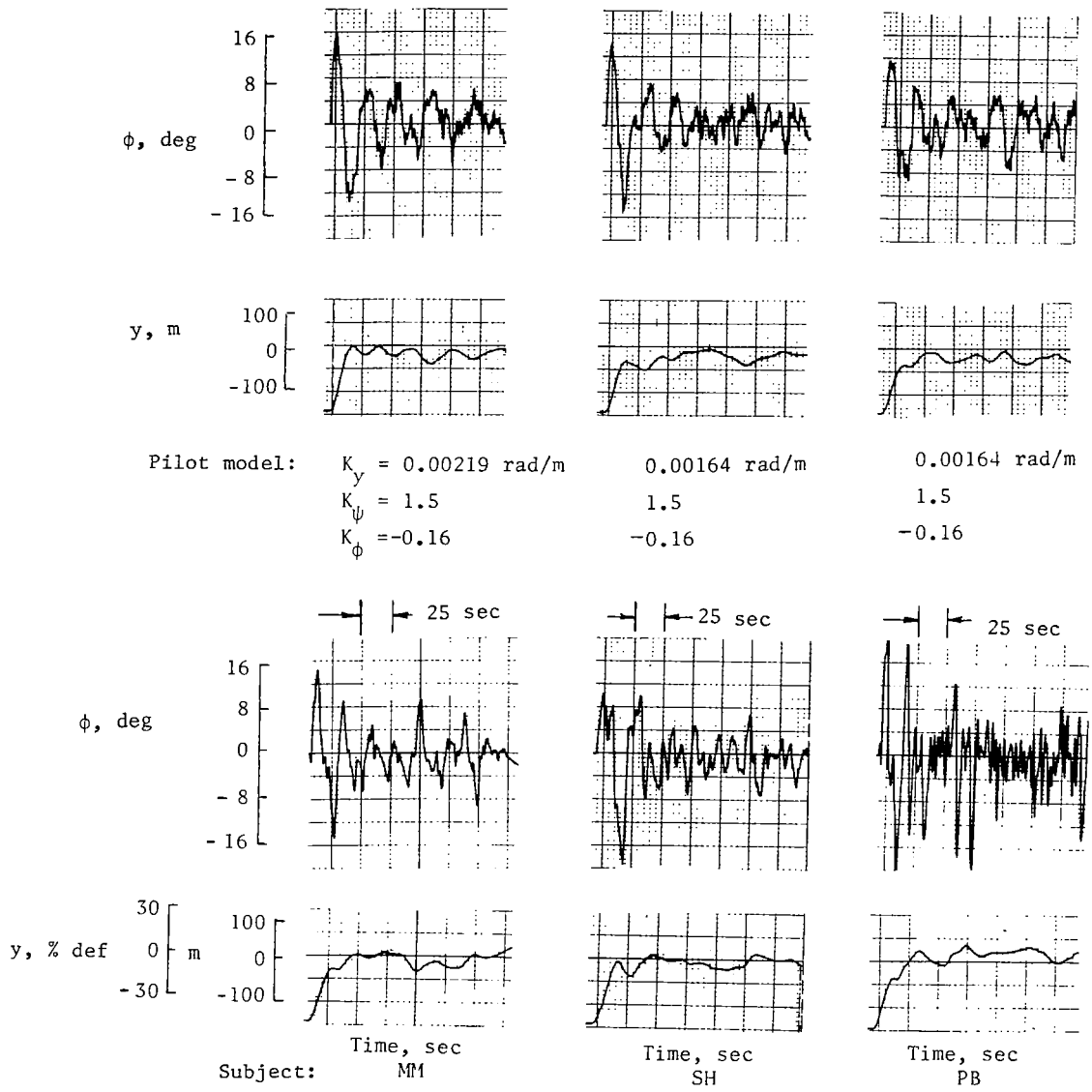

(a) CDI.

Figure 12.- Responses with ILS station at 5 n. mi. range.

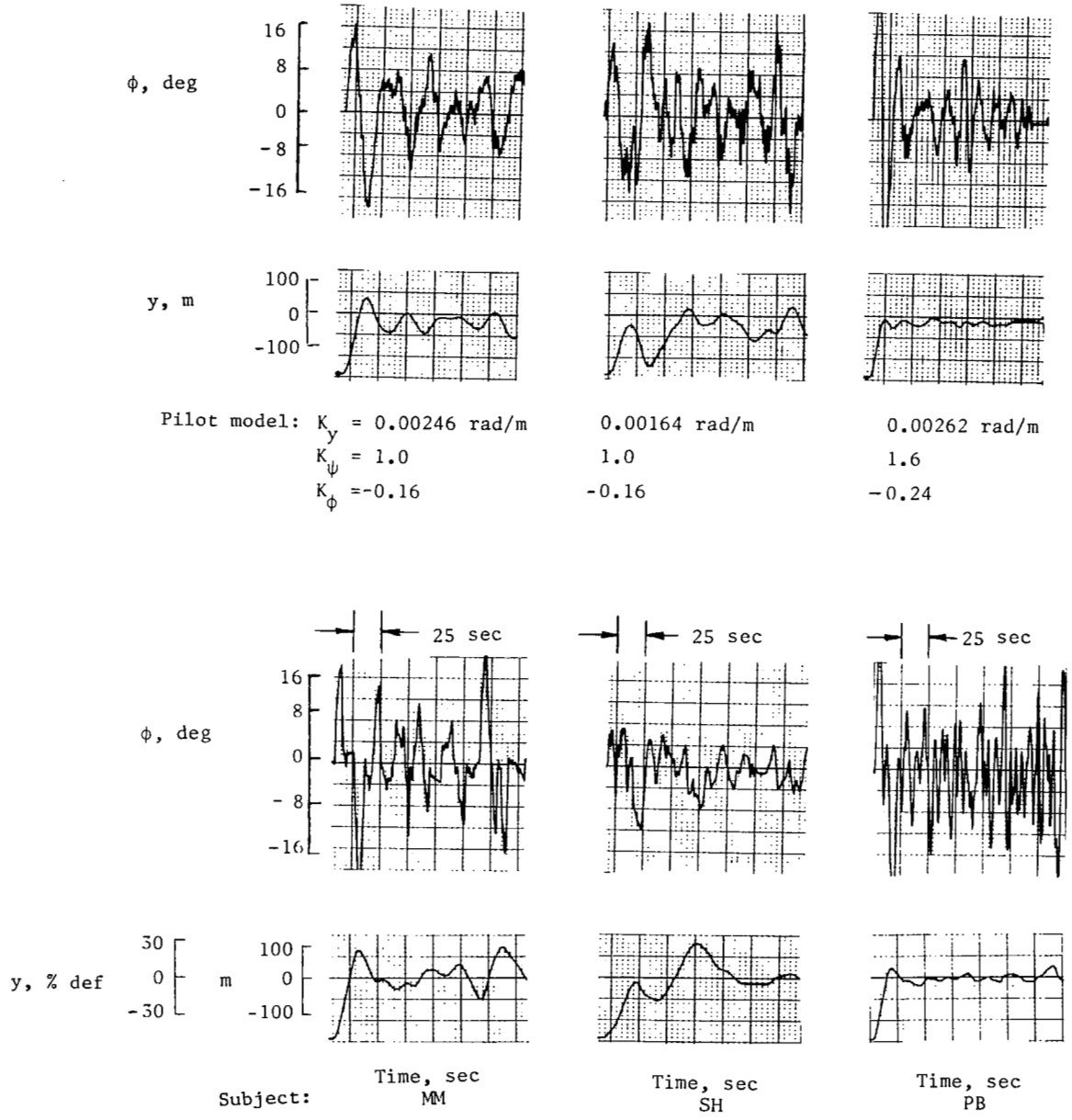

(b) HSI.

Figure 12.- Concluded.

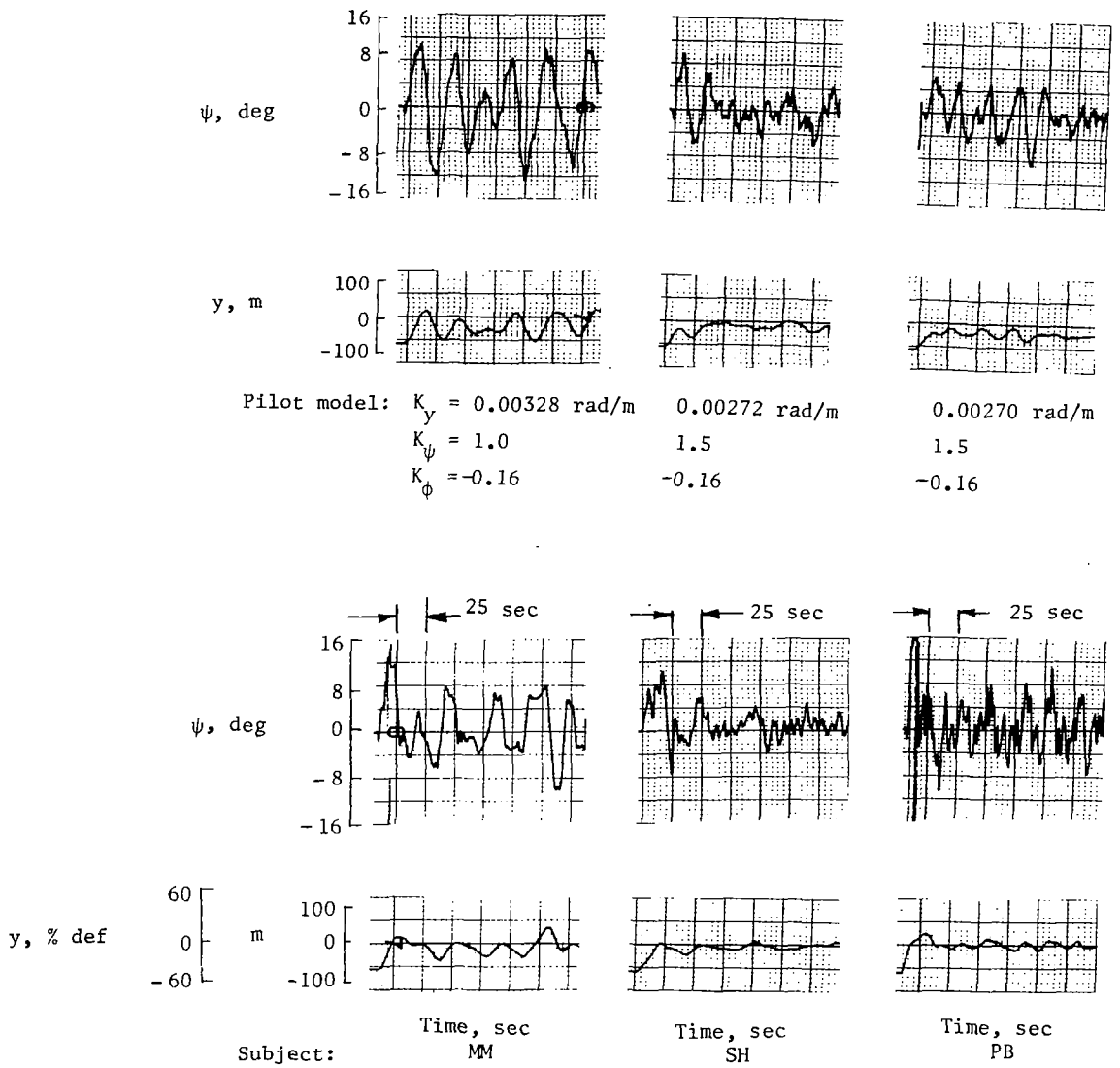

(a) CDI.

Figure 13.- Responses with ILS station at 1.25 n. mi. range.

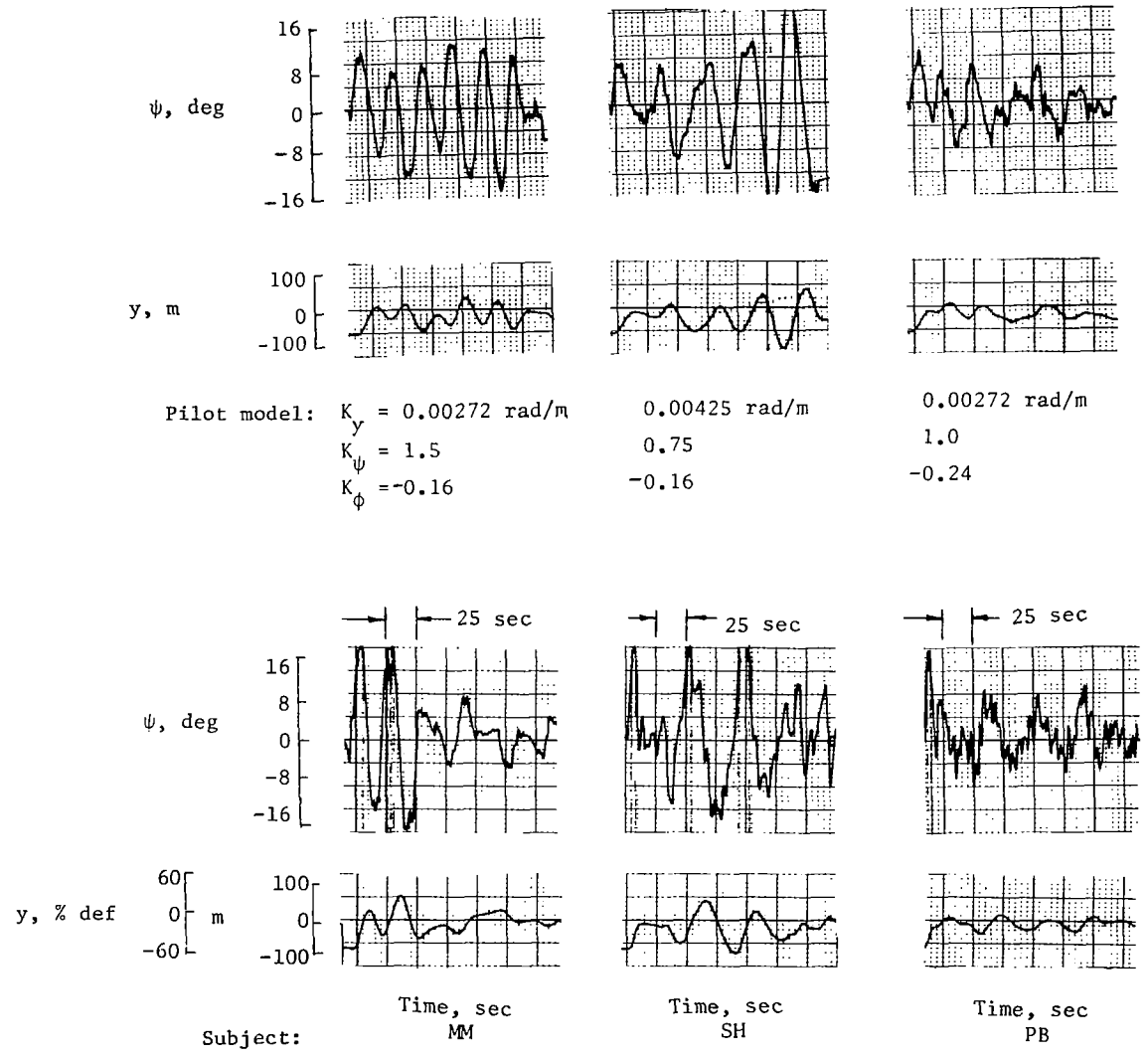

(b) HSI.

Figure 13.- Concluded.

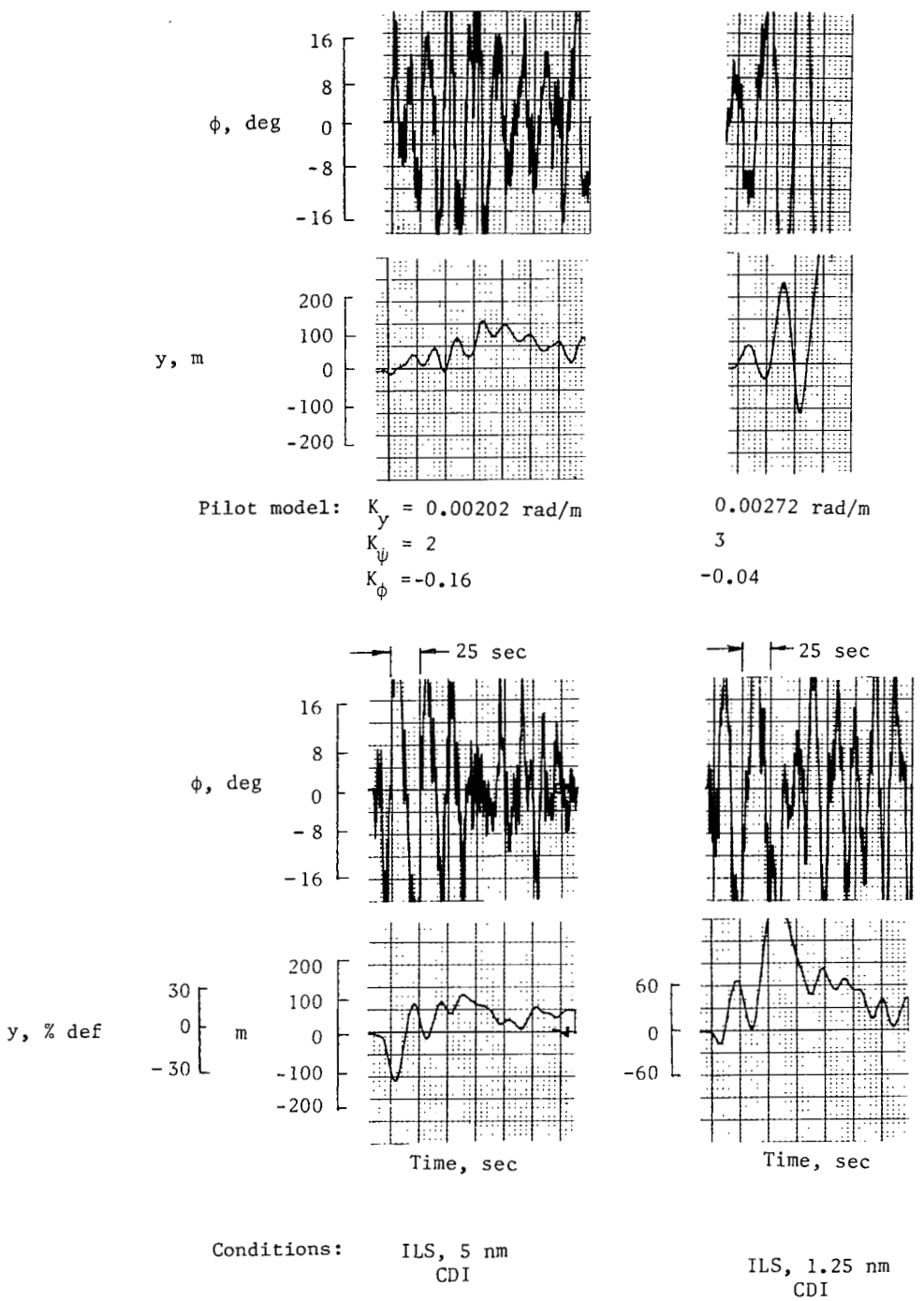

Figure 14.- Responses with wind disturbances for subject MM.

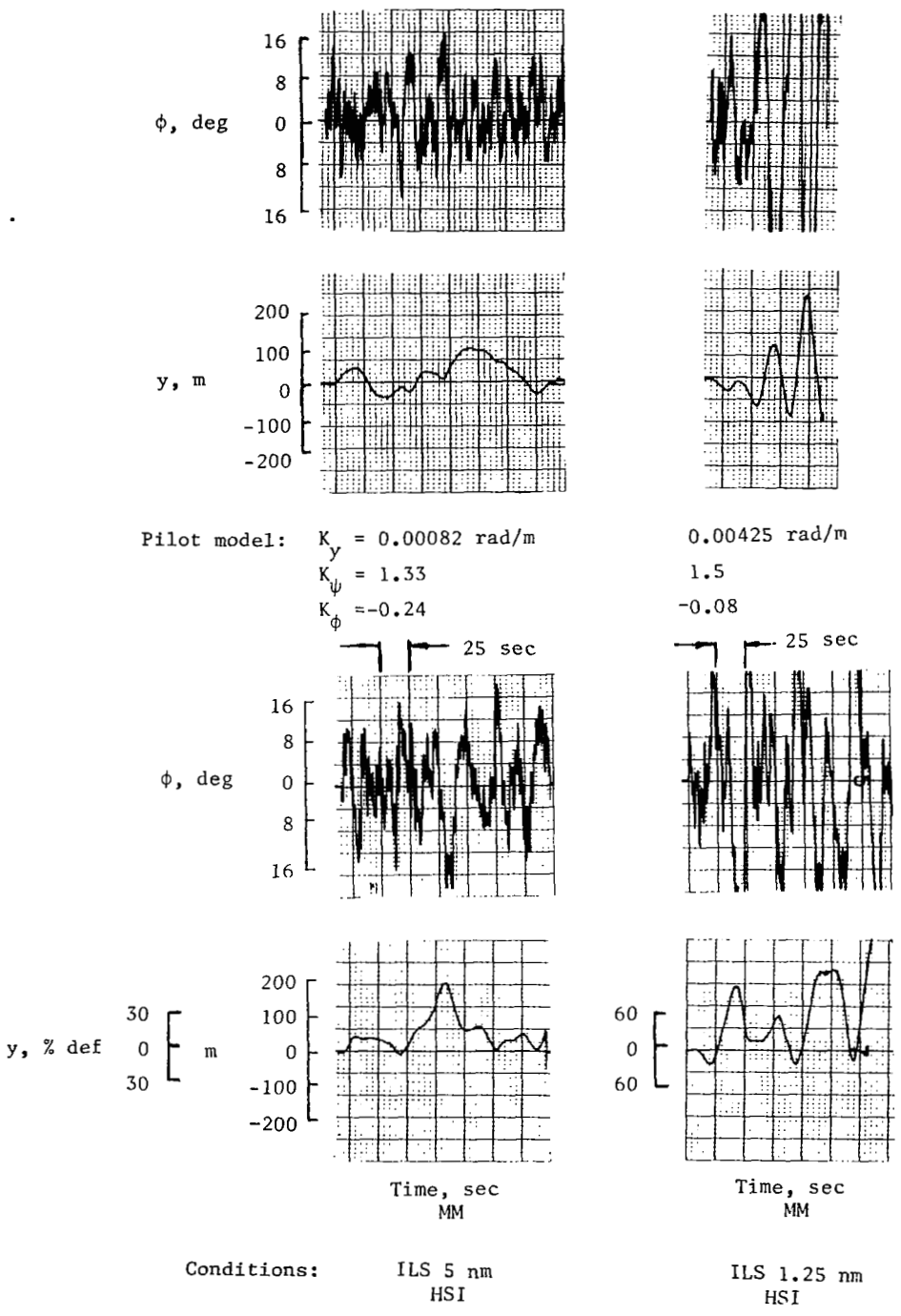

Figure 14.- Concluded.

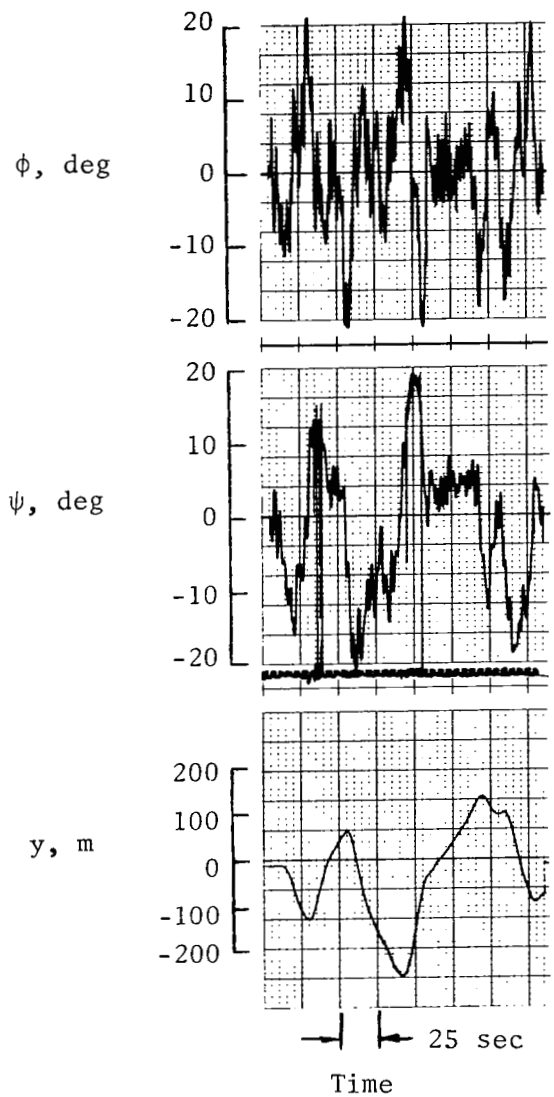

Figure 15.- Sample divergence stopped after $1\frac{1}{2}$ cycles for subject JR.

1. Report No.	2. Government Accession No.	3. Recipient's Catalog No.
NASA TP-1776		

4. Title and Subtitle	5. Report Date
SIMULATOR STUDY OF CONVENTIONAL GENERAL AVIATION INSTRUMENT DISPLAYS IN PATH-FOLLOWING TASKS WITH EMPHASIS ON PILOT-INDUCED OSCILLATIONS	December 1980
	6. Performing Organization Code 505-41-73-01

7. Author(s)	8. Performing Organization Report No.
James J. Adams	L-13785
	10. Work Unit No.

9. Performing Organization Name and Address	11. Contract or Grant No.
NASA Langley Research Center Hampton, VA 23665	
	13. Type of Report and Period Covered
12. Sponsoring Agency Name and Address	Technical Paper
National Aeronautics and Space Administration Washington, DC 20546	14. Sponsoring Agency Code

15. Supplementary Notes

16. Abstract

A study of the use of conventional general aviation instruments by general aviation pilots in a six-degree-of-freedom, fixed-base simulator has been conducted. The tasks performed were tracking a VOR radial and making an ILS approach to landing. A special feature of the tests was that the sensitivity of the displacement indicating instruments (the RMI, CDI, and HSI) was kept constant at values corresponding to 5 n. mi. and 1.25 n. mi. from the station. Both statistical and pilot-model analyses of the data were made. The results show that performance in path following improved with increases in display sensitivity up to the highest sensitivity tested. At this maximum test sensitivity, which corresponds to the sensitivity existing at 1.25 n. mi. from the ILS glide slope transmitter, tracking accuracy was no better than it was at 5 n. mi. from the station and the pilot-aircraft system exhibited a marked reduction in damping. In some cases, a pilot-induced, long-period unstable oscillation occurred.

17. Key Words (Suggested by Author(s))	18. Distribution Statement
Aircraft display Pilot induced oscillations Pilot models Lateral control	Unclassified - Unlimited Subject Category 06

19. Security Classif. (of this report)	20. Security Classif. (of this page)	21. No. of Pages	22. Price
Unclassified	Unclassified	52	A04

For sale by the National Technical Information Service, Springfield, Virginia 22161

NASA-Langley, 1980